LA-13118

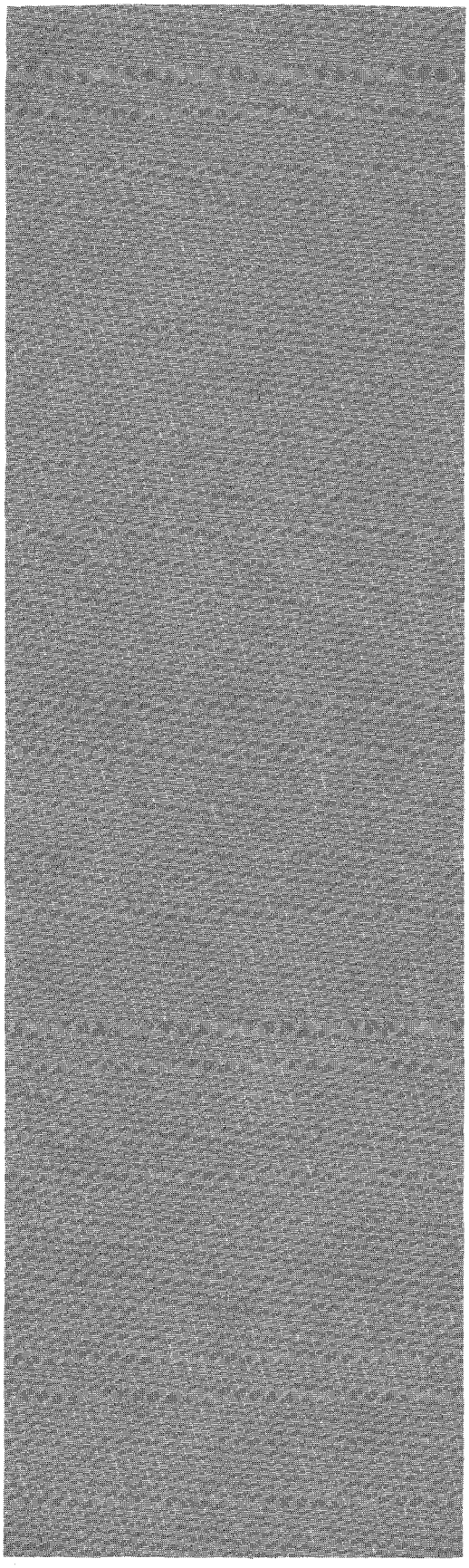

General-Purpose Heat Source: Research and Development Program

Cold-Process Verification Test Series

Los Alamos
NATIONAL LABORATORY

Los Alamos National Laboratory is operated by the University of California for the United States Department of Energy under contract W-7405-ENG-36.

Edited by Jennifer Graham, Group CIC-1
Photocomposition by Wendy Burditt, Group CIC-1

This work was supported by the U.S. Department of Energy, Office of Nuclear Energy, Office of Special Applications.

An Affirmative Action/Equal Opportunity Employer

DISCLAIMER

LA-13118

UC-500
Issued: June 1996

General-Purpose Heat Source: Research and Development Program

Cold-Process Verification Test Series

M. A. H. Reimus
T. G. George

Los Alamos
NATIONAL LABORATORY
Los Alamos, New Mexico 87545

GENERAL-PURPOSE HEAT SOURCE: RESEARCH AND DEVELOPMENT PROGRAM

Cold-Process Verification Test Series

by

M. A. H. Reimus and T. G. George

ABSTRACT

The General-Purpose Heat Source (GPHS) provides power for space missions by transmitting the heat of ^{238}Pu decay to an array of thermoelectric elements. Because any space mission could experience a launch abort or return from orbit, the heat source must be designed and constructed to survive credible accident environments. Previous testing conducted in support of the Galileo and Ulysses missions documented the response of GPHSs and individual GPHS capsules fueled with $^{238}UO_2$ (^{235}U-depleted) to a variety of explosive overpressure and impact events. In the early 1990s, Los Alamos National Laboratory (LANL) resumed fabrication of $^{238}UO_2$ GPHS pellets. The Cold-Process Verification (CPV) Test Series was designed to compare the response of GPHS heat sources loaded with recently fabricated hot- and cold-pressed $^{238}UO_2$ pellets to the response of urania pellets used in the Galileo and Ulysses performance tests. This report documents eleven bare-capsule impacts and one impact of a fully loaded GPHS module. All of the failures observed in the bare-clad impact tests were similar to failures observed in previous safety tests. No failures occurred in the module impact test.

I. INTRODUCTION

The General-Purpose Heat Source (GPHS) is a modular component of the radioisotope thermoelectric generators (RTGs) that will provide power for National Aeronautics and Space Administration's (NASA's) Cassini mission to Saturn. An RTG generates electric power by using the heat of ^{238}Pu α-decay to create a temperature differential across a thermoelectric array. Each RTG is loaded with 18 GPHS modules, and each GPHS module (Fig. 1) contains four $^{238}PuO_2$ fuel pellets that provide a total thermal output of 250 W. Each fuel pellet is encapsulated in a vented, DOP-26 iridium alloy shell. Two capsules are held in a Fineweave-

Pierced Fabric* (FWPF) graphite impact shell (GIS), and two GISs are contained within a FWPF aeroshell.

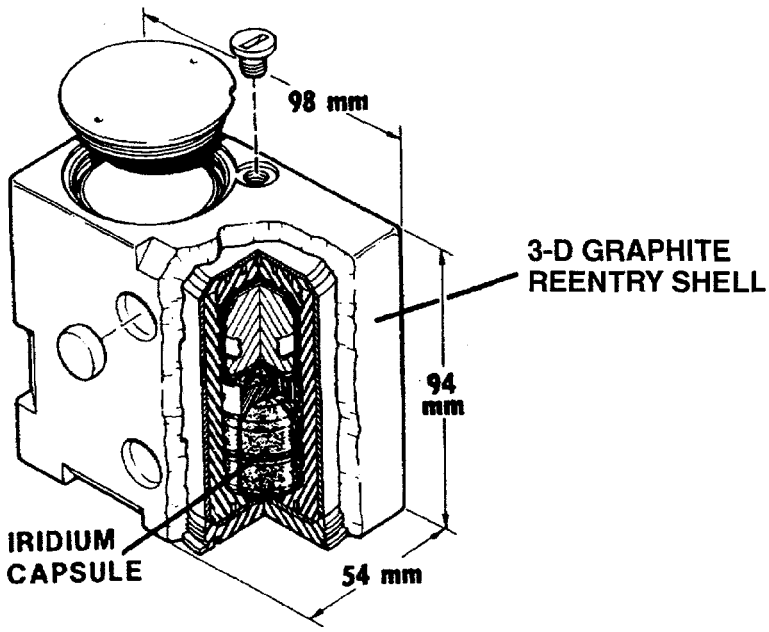

Fig. 1. GPHS Module.

Because any space mission could experience a launch abort or return from orbit, the GPHS heat source has been designed and constructed to survive credible accident environments. Previous testing conducted in support of the Galileo and Ulysses missions documented the response of the GPHS heat source to a variety of fragment-impact, aging, atmospheric reentry, and Earth impact conditions.[1-8] Tests that required field testing of heat source and RTG components (such as solid-propellent fire, explosive overpressure, and large-fragment interaction) were performed using GPHS capsules fueled with $^{238}UO_2$ (^{235}U-depleted).[9-13]

In the early 1990s, Los Alamos National Laboratory (LANL) resumed fabrication of $^{238}UO_2$ GPHS pellets. The Cold-Process Verification (CPV) Test Series was formulated to compare the response of GPHS heat sources loaded with recently fabricated hot- and cold-pressed $^{238}UO_2$ pellets to the response of urania pellets used in the Galileo and Ulysses performance tests. This report documents eleven bare-capsule impacts and one impact of a fully loaded GPHS module.

II. BACKGROUND

A. Fabrication of Urania Pellets

The depleted urania pellets used in this study were fabricated from urania powder produced by Oak Ridge National Laboratory (urania lot # NF-30-4225). Five of the pellets used were fabricated by hot pressing, and the remaining pellets were cold pressed and sintered. Both fabrication techniques are described in more detail in the following sections.

1. Cold-Pressed and Sintered Pellets. The urania powder was mixed with a solution of cetyl alcohol (binder) dissolved in acetone. The amount of cetyl alcohol used was approximately 2% of the weight of urania powder. The amount of acetone used was 0.25 mL per gram of urania. The urania/alcohol mixture was gently heated with a heat lamp and blended until dry. This material was then passed through a 30-mesh sieve to break up any agglomerates. The material was then isostatically pressed at 25 to 30 Ksi and then crushed and passed through a 60-mesh sieve.

*Fineweave-Pierced Fabric 3-D carbon/carbon composite, a product of AVCO Systens Division, 201 Lowell St., Wilmington, MA 01887.

After sieving, approximately 150 g of the treated urania were loaded into a graphite die and then pressed in a Carver 25-ton press for 1 min at 20 tons of load. The rough pellet was then removed and sintered at 1825°C for 4 hr in dry H_2 (45°F dewpoint). The pellet was ground to final dimensions and then vacuum outgassed at 250°C for 2 hr.

2. Hot-Pressed Pellets. A graphite die was loaded with the appropriate amount of untreated urania powder and then pressed to 600 psi at ambient temperature. The pressure and temperature were then ramped up to end points of 3000 psi and 1600°C. Once the desired pressure and temperature set points were reached, the load was held under these conditions for 10 min. The pressure was then lowered to 2000 psi, and the load was allowed to cool to ambient temperature, for approximately 12 hr. When ambient temperature was reached, the pressure was released and the pressed pellet was ejected from the die. The pellet was inspected for cracks and densification and then ground and vacuum outgassed in the same manner as the cold-pressed and sintered pellets.

B. Source and History of Graphite Components Used in CPV-12

The graphite components used in the single-module impact in the CPV test series, CPV-12, were obtained from EG&G Mound Applied Technologies (EG&G MAT). Components of the GPHS module are identified in Table I.

TABLE I. CPV-12 Module Components

Component	**ID**
Module	84
A GIS Assembly	
Insulating Sleeve	B48-1
GIS	PGL-167
Floating Membrane	PFL-167
GPHS, Open End	SC0073
GPHS, Blind End	SC0072
C GIS Assembly	
Insulating Sleeve	B48-2
GIS	PGL-168
Floating Membrane	PFL-168
GPHS, Open End	SC0075
GPHS, Blind End	SC0074

III. EXPERIMENTAL PROCEDURES

A. Pretest Data

The dimensions and weights of the urania pellets were measured and recorded before encapsulation. After the pellets were encapsulated in iridium-clad vent sets, the dimensions of the clads were recorded. The clads were then submitted for ultrasonic testing (UT) of the girth weld. Table II lists the dimensions and process history of the the urania pellets used in this study. Table III lists the clad vent sets and the dimensions of the simulant-fueled GPHSs used in this study. Table IV lists the UT results.

TABLE II. Urania Pellet Process History and Dimensions

Test ID	Clad ID	Pellet ID	Fabrication Method	Ave. Diameter (in.)[a]	Length (in.)	Weight (g)
CPV-1	SC0011	92-27	HP[b]	1.090	1.091	145.7
CPV-2	SC0008	92-43	HP	1.090	1.095	145.9
CPV-3	SC0004	SD431-9	CP[c]	1.089	1.090	136.7
CPV-4	SC0020	CDI-4	CP	1.087	1.090	145.5
CPV-5	SC0017	CDI-6	CP	1.085	1.092	143.1
CPV-6	SC0018	CDI-11	CP	1.086	1.092	146.7
CPV-7	SC0019	CDI-10	CP	1.085	1.091	146.4
CPV-8	SC0006	D431-9-4	CP	1.089	1.091	130.5
CPV-9	SC0015	92-26	HP	1.088	1.095	146.2
CPV-10	SC0009	92-36	HP	1.087	1.092	143.9
CPV-11	SC0016	92-44	HP	1.090	1.090	146.2
CPV-12	SC0072	8	CP	1.089	1.089	145.3
CPV-12	SC0073	11	CP	1.090	1.090	145.8
CPV-12	SC0074	12	CP	1.089	1.089	145.3
CPV-12	SC0075	14	CP	1.089	1.090	146.9

[a]Average of three measurements.
[b]HP: hot presssed.
[c]CP: cold pressed and sintered.

TABLE III. Cold-Process Verification Test Capsules

Clad	Test	PICS[a] No.	Vent cup Diameter (in.)	Weld Diameter (in.)	Shield Cup Diameter (in.)	Length (in.)
SC0011	CPV-1	SR-35	ND[b]	ND	ND	ND
SC0008	CPV-2	9808-00-1481	1.163	1.175	1.163	1.176
SC0004	CPV-3	9808-00-1483	1.165	1.167	1.167	1.184
SC0020	CPV-4	SR-23	1.164	1.174	1.167	1.178
SC0017	CPV-5	9808-00-1490	1.168	1.173	1.167	1.178
SC0018	CPV-6	9808-00-1405	1.169	1.174	1.168	1.180
SC0019	CPV-7	SR-22	1.167	1.175	1.168	1.179
SC0006	CPV-8	9808-00-1428	1.169	1.174	1.170	1.180
SC0015	CPV-9	9808-00-1404	1.169	1.170	1.170	1.181
SC0009	CPV-10	9808-00-1400	1.170	1.172	1.170	1.181
SC0016	CPV-11	SR-13	1.169	1.174	1.168	1.180
SC0072	CPV-12	9808-01-2162	ND	ND	ND	ND
SC0073	CPV-12	9808-01-2163	ND	ND	ND	ND
SC0074	CPV-12	9808-01-2165	ND	ND	ND	ND
SC0075	CPV-12	9801-01-2166	ND	ND	ND	ND

[a]Post-impact containment shell.
[b]Not determined.

TABLE IV. CPV GPHS UT Results

Test ID	Clad ID	Max UT Ind. (Equiv. mils)	Location (deg[a])	UT Capsule Disposition
CPV-1	SC0011	7.8	142	Reject
CPV-2	SC0008	5.8	18	Reject
		6.9	24	
CPV-3	SC0004	3.9	14	Accept
CPV-4	SC0020	5.4	26	Reject
CPV-5	SC0017	6.7	6	Reject
		7.5	68	
CPV-6	SC0018	5.4	21	Reject
CPV-7	SC0019	5.1	40	Reject
		5.3	41	
CPV-8	SC0006	4.2	158	Accept
CPV-9	SC0015	5.7	14	Reject
		5.9	256	
CPV-10	SC0009	5.8	279	Reject
CPV-11	SC0016	4.8	276	Accept
CPV-12	SC0072	2.7	134	Accept
CPV-12	SC0073	2.4	92	Accept
CPV-12	SC0074	3.1	280	Accept
CPV-12	SC0075	2.5	84	Accept

[a]Angular location referenced to the weld start at 0 deg.

B. Impact Testing

Two types of impact tests were conducted: bare-clad and full-module. The clads impacted in the bare-clad tests, CPV-1 through CPV-11, were placed on a support cradle fabricated of molybdenum sheet. This support cradle was designed to hold the clad in the desired impact orientation (with the axis of the clad parallel to the target) and was outgassed in a vacuum furnace at 900°C for 1 hr before use. The cradle was placed in a tantalum can (previously outgassed under the same conditions as the support cradle) and welded shut in an inert atmosphere. The can was evacuated and backfilled with He to approximately 3 psia through a port in the bottom of the can and then sealed. The can was transported to the Los Alamos Isotope Fuels Impact Test (IFIT) Facility. Once loaded, the test components were heated to the desired temperature and then impacted against a hardened steel plate. The temperature of the clad was monitored by means of a thermocouple contacting the side of the can. The specific test conditions for each test are given in Table V.

In the full module test, CPV-12, a graphite module loaded with four capsules was impacted against a steel plate. The clads were loaded into two graphite impact shells (GISs) then placed into the graphite module. A hole was drilled through the module, and a thermocouple was placed in contact with an iridium clad. The thermocouple was secured by wrapping a tantalum wire spring around the thermocouple insulation and the module. The module was then installed in a self-sealing catch tube in the IFIT, heated to temperature, and impacted against a hardened steel plate. The specific test conditions are given in Table V.

TABLE V. CPV Test Parameters

Test ID	Hot-/Cold-Pressed	Test Type	Impact Orientation[a]	Velocity (m/s)	Temperature (°C)
CPV-1	Hot	Bare Clad	A	55.0 ± 1.0	1092
CPV-2	Hot	Bare Clad	A	55.0 ± 1.0	1090
CPV-3	Cold	Bare Clad	A	55.0 ± 0.1	1090
CPV-4	Cold	Bare Clad	A	55.2 ± 0.2	1090
CPV-5	Cold	Bare Clad	A	55.3 ± 0.1	1090
CPV-6	Cold	Bare Clad	A	55.0 ± 0.1	1090
CPV-7	Cold	Bare Clad	A	55.3 ± 0.1	1090
CPV-8	Cold	Bare Clad	A	55.3 ± 0.4	1090
CPV-9	Hot	Bare Clad	A	54.5 ± 0.04	1090
CPV-10	Hot	Bare Clad	A	55.5 ± 0.05	1090
CPV-11	Hot	Bare Clad	B	54.8 ± 0.08	1090
CPV-12	Cold	Module	C	54.4 ± 0.07	970

[a]A = Capsule equator perpendicular to target; side-on impact
B = Capsule equator parallel to target; end-on impact
C = Module flight control surface parallel to target; side-on impact (flight control surface was impact face)

C. Post-Impact Evaluation

After each impact test, the interior atmosphere of the sealed catch tube containing the clad/ module was monitored for radioactive activity though a side port. The test components were removed from the catch tube. If any urania was detected, the catch tube was rinsed and the fines collected. The tantalum can containing the bare clad was opened and its interior swiped for activity. Fines were collected by rinsing the can interior and collecting the resulting liquid in a separate container. All test components were photographed, and the clads were measured to determine post-impact capsule strains. The size and location of all clad failures and cracks were recorded.

After macroscopic examination, the clads were opened and the patterns of fuel fracture were photographed. All of the bare-clad impacted clads were then defueled and the fuel was submitted for particle size analysis. Only the fuel from the most severely strained clad recovered in the full-module impact test, CPV-12, was submitted for particle size analysis.

The iridium clads were sampled to provide specimens for metallographic analysis. All capsules used in bare-clad impacts were sampled; only the most severely strained clad recovered from CPV-12 was sampled. At a minimum, the following metallographic sections were taken from each clad: axial sections of the vent and shield cup walls, vent cross section, and cross sections of single-pass weld and weld overlap regions. All clad failures and areas of severe localized deformation were sectioned for metallographic examination.

IV. RESULTS

The individual tests and postmortem examinations are summarized below. The analytical results are tabulated as follows:

Table VI. CPV Test Summaries

Table VII. Particle Size Analysis of CPV-1, CPV-2, and CPV-3

Table VIII. Particle Size Analysis of CPV- 4 through CPV-7

Table IX. Particle Size Analysis of CPV-8 through CPV-12

Table X. CPV Test Series - Cup Wall Microstructure

Table XI. CPV Test Series - UT Results and Failure Locations

Table VI. CPV Test Summaries

	STRAIN MINIMUM (%)					STRAIN MAXIMUM (%)					
Test ID	**Clad ID**	**Axial, length**	**Vent Cup**	**Weld**	**Shield Cup**	**Axial, length**	**Vent Cup**	**Weld**	**Shield Cup**	**Num. of Failures**	**Amount of Urania Released (g)**
CPV-1	SC0011	+2.1	-10.3[a]	-10.7[a]	-11.2[a]	+15.5	+10.3[a]	+14.8[a]	+7.0[a]	3	0.0415
CPV-2	SC0008	+9.5	-16.3	-16.1	-12.9	+17.1	+17.8	+18.5	+9.3	0	None
CPV-3	SC0004	+0.84	-12.8	-13.5	-13.6	+14.3	+6.9	+9.3	+7.6	0	None
CPV-4	SC0020	-0.9	-8.9	-8.9	-10.8	+16.1	+6.6	+8.3	+5.7	1	0.1030
CPV-5	SC0017	+3.1	-16.1	-11.3	-11.3	+15.2	+8.3	+9.4	+6.0	2	NM[b]
CPV-6	SC0018	+3.6	-12.2	-8.9	-9.9	+15.2	+5.8	+6.3	+4.3	1	None
CPV-7	SC0019	+0.7	-11.4	-11.2	-10.5	+14.3	+5.8	+7.8	+6.3	2	None
CPV-8	SC0006	+3.7	-9.2	-5.2	-4.7	+12.8	+6.9	+6.9	+6.8	0	None
CPV-9	SC0015	+0.1	-11.0	-9.0	-12.0	+13.8	+6.5	+8.1	+6.0	3	NM[b]
CPV-10	SC0009	-1.2	-10.6	-9.0	-10.0	+12.4	+5.6	+8.2	+8.4	2	None
CPV-11	SC0016	-13.6	+10.2	+5.2	+8.8	-7.0	+3.5	+9.9	+12.2	3	None
CPV-12	SC0072	ND[a]	-1.5[a]	-3.0[a]	-2.0[a]	+1.8[a]	+5.0[a]	+5.4[a]	+5.0[a]	0	None
CPV-12	SC0073	ND[a]	-3.0[a]	-4.7[a]	-1.8[a]	+3.9[a]	+4.7[a]	+6.5[a]	+3.1[a]	0	None
CPV-12	SC0074	ND[a]	-2.9[a]	-5.8[a]	-3.5[a]	+3.0[a]	+5.5[a]	+6.6[a]	+5.3[a]	0	None
CPV-12	SC0075	ND[a]	-3.7[a]	-5.9[a]	-3.7[a]	+3.6[a]	+4.8[a]	+5.5[a]	+4.1[a]	0	None

[a]Pretest diametrical measurements were not obtained; calculated diametral strains are based on nominal cup wall and weld diameters of 1.168 and 1.173 in. respectively; calculated axial strains are based on nominal length of 1.178 in.

[b]Release quantity was too small to be weighed or sampled for particle size analysis.

Table VII. Particle Size Analysis of CPV-1, CPV-2, and CPV-3

Particle Size Range (μm)	CPV-1 (SC0011) Retained Fuel	CPV-1 (SC0011) Released Fuel[a]	CPV-2 (SC0008) Retained Fuel	CPV-3 (SC0004) Retained Fuel
+5600	0.3766	0.0000	0.5293	0.4189
+2000 to 5600	0.3310	0.0000	0.2947	0.3054
+850 to 2000	0.1823	0.0000	0.0354	0.1687
+425 to 850	0.0108	0.0000	0.1131	0.0418
+180 to 425	0.0495	0.0000	0.0135	0.0257
+125 to 180	0.0225	0.0000	0.0016	0.0033
+75 to 125	0.0026	0.0000	0.0016	0.0046
+45 to 75	0.0018	0.0000	0.0016	0.0022
+30 to 45	0.0009	0.0104	0.0000	0.0007
+20 to 30	0.0014	0.0475	0.0000	0.0020
+10 to 20	0.0047	0.1599	0.0006	0.0083
+9 to 10	0.0006	0.0341	0.0004	0.0016
+8 to 9	0.0007	0.0263	0.0005	0.0015
+7 to 8	0.0008	0.0426	0.0006	0.0018
+6 to 7	0.0012	0.0940	0.0011	0.0029
+5 to 6	0.0015	0.1257	0.0014	0.0036
+4 to 5	0.0017	0.1494	0.0014	0.0035
+3 to 4	0.0018	0.1211	0.0012	0.0020
+2 to 3	0.0017	0.0705	0.0007	0.0009
+1 to 2	0.0048	0.0937	0.0010	0.0005
<1	0.0011	0.0248	0.0003	0.0001
Total:	1.0000	1.0000	1.0000	1.0000
Weight fraction <10 μm:	0.0159	0.7822	0.0086	0.0184

[a]0.0415 g released.

Table VIII. Particle Size Analysis of CPV- 4 through CPV-7

Particle Size Range (μm)	CPV-4 (SC0020) Retained Fuel	CPV-4 (SC0020) Released Fuel[a]	CPV-5 (SC0017) Retained Fuel	CPV-6 (SC0018) Retained Fuel	CPV-7 (SC0019) Retained Fuel
+5600	0.3850	0.0000	0.3952	0.2526	0.3667
+2000 to 5600	0.2439	0.0000	0.3482	0.3041	0.3186
+850 to 2000	0.2669	0.0000	0.1504	0.2551	0.1870
+425 to 850	0.0366	0.0000	0.0556	0.1082	0.0636
+180 to 425	0.0357	0.0000	0.0178	0.0511	0.0334
+125 to 180	0.0065	0.0000	0.0039	0.0060	0.0068
+75 to 125	0.0071	0.0156	0.0040	0.0081	0.0045
+45 to 75	0.0054	0.1471	0.0031	0.0056	0.0059
+30 to 45	0.0001	0.1433	0.0006	0.0006	0.0018
+20 to 30	0.0001	0.0646	0.0017	0.0011	0.0024
+10 to 20	0.0014	0.1848	0.0073	0.0031	0.0045
+9 to 10	0.0003	0.0202	0.0013	0.0004	0.0004
+8 to 9	0.0003	0.0117	0.0011	0.0004	0.0004
+7 to 8	0.0005	0.0166	0.0013	0.0004	0.0004
+6 to 7	0.0010	0.0210	0.0019	0.0005	0.0007
+5 to 6	0.0016	0.0472	0.0023	0.0007	0.0008
+4 to 5	0.0020	0.0618	0.0019	0.0007	0.0008
+3 to 4	0.0016	0.0530	0.0013	0.0005	0.0006
+2 to 3	0.0012	0.0443	0.0005	0.0003	0.0003
+1 to 2	0.0022	0.1357	0.0005	0.0004	0.0004
<1	0.0006	0.0331	0.0001	0.0001	0.0000
Total:	1.0000	1.0000	1.0000	1.0000	1.0000
Weight fraction <10 μm:	0.0113	0.4446	0.0122	0.0044	0.0048

[a]0.103 g released.

Table IX. Particle Size Analysis of CPV-8 through CPV-12

Particle Size Range (μm)	CPV-8 (SC0006) Fuel	CPV-9 (SC0015) Retained Fuel	CPV-10 (SC0009) Retained Fuel	CPV-11 (SC0016) Retained Fuel	CPV-12 (SC0074) Fuel
+5600	0.5154	0.2482	0.3854	0.6278	0.5805
+2000 to 5600	0.3056	0.4551	0.3657	0.1774	0.2888
+850 to 2000	0.1141	0.2075	0.1758	0.1251	0.0893
+425 to 850	0.0311	0.0552	0.0436	0.0422	0.0258
+180 to 425	0.0134	0.0216	0.0156	0.0178	0.0102
+125 to 180	0.0019	0.0026	0.0031	0.0018	0.0018
+75 to 125	0.0021	0.0018	0.0017	0.0011	0.0015
+45 to 75	0.0011	0.0016	0.0014	0.0013	0.0011
+30 to 45	0.0012	0.0000	0.0000	0.0000	0.0001
+20 to 30	0.0018	0.0000	0.0000	0.0000	0.0002
+10 to 20	0.0052	0.0003	0.0010	0.0002	0.0003
+9 to 10	0.0005	0.0002	0.0003	0.0001	0.0000
+8 to 9	0.0006	0.0001	0.0004	0.0001	0.0000
+7 to 8	0.0007	0.0002	0.0005	0.0002	0.0000
+6 to 7	0.0009	0.0004	0.0009	0.0003	0.0000
+5 to 6	0.0012	0.0006	0.0011	0.0003	0.0001
+4 to 5	0.0013	0.0007	0.0012	0.0005	0.0001
+3 to 4	0.0009	0.0007	0.0010	0.0006	0.0002
+2 to 3	0.0005	0.0007	0.0005	0.0005	0.0000
+1 to 2	0.0004	0.0018	0.0007	0.0017	0.0000
<1	0.0001	0.0007	0.0001	0.0010	0.0000
Total:	1.0000	1.0000	1.0000	1.0000	1.0000
Weight fraction <10 μm:	0.0071	0.0061	0.0067	0.0053	0.0004

Table X. CPV Test Series - Cup Wall Microstructure

Test	Clad ID	Iridium Cup	Average no. grains/ 0.65 mm nominal wall thickness		Comments
			Axial	Transverse	
CPV-1	SC0011	Z511-3	ND[a]	23	Typical microstructure
		Z514-4	ND	42	Unusual small grains
CPV-2	SC0008	9753-00-1806	25	25	Isolated large exterior grains
		9754-00-2094	22	25	Typical microstructure
CPV-3	SC0004	9753-00-1810	25	22	Typical microstructure
		9754-00-2304	22	23	Typical microstructure
CPV-4	SC0020	X342-2	22	ND	Typical microstructure
		YR-421-1	22	ND	Typical microstructure
CPV-5	SC0017	9753-00-1817	23	ND	Typical microstructure
		9754-00-2097	23	ND	Typical microstructure
CPV-6	SC0018	9753-00-1523	25	ND	Typical microstructure
		9754-00-2025	23	ND	Typical microstructure
CPV-7	SC0019	X340-4	ND	ND	Typical microstructure
		YR427-6	17	ND	Typical microstructure
CPV-8	SC0006	9753-00-1524	20	ND	Typical microstructure
		9754-00-2021	22	ND	Typical microstructure
CPV-9	SC0015	9753-00-1522	22	ND	Typical microstructure
		9754-00-2024	19	ND	Typical microstructure
CPV-10	SC0009	9753-00-1508	22	ND	Typical microstructure
		9754-00-2007	22	ND	Typical microstructure
CPV-11	SC0016	X312-2	15	ND	Typical microstructure
		XR367-2	29	ND	Typical microstructure
CPV-12	SC0074	9753-01-3004	26	27	Typical microstructure
		3625-01-3504	26	26	Typical microstructure

[a]Not determined.

Table XI. CPV Test Series - Capsule UT Results and Location of Weld Failures

	Max UT Ind.			Weld Crack	
Capsule ID	Equiv.	mils	Location (deg.)[a]	Location(s)[a]	Comments
SC0011 (CPV-1)	7.8		142	300	Breach with urania release, wall offset at approximately 144 deg.
SC0008 (CPV-2)	5.8 6.9		18 24	None	None
SC0004 (CPV-3)	3.9		14	None	None
SC0020 (CPV-4)	5.4		26	120	Axial crack extended from shield cup, through weld,and into vent cup.
SC0017 (CPV-5)	6.7 7.5		6 68	90	Axial crack extended from vent cup, through weld, and into shield cup.
SC0018 (CPV-6)	5.4		21	None	None
SC0019 (CPV-7)	5.1 5.3		40 41	300 - 45	Weld centerline crack, no urania release.
SC0006 (CPV-8)	4.2		158	None	None
SC0015 (CPV-9)	5.7 5.9		14 256	210	Axial crack extended from weld centerline into vent cup.
SC0009 (CPV-10)	5.8		279	315	Axial crack transected weld.
SC0016 (CPV-11)	4.8		276 245	270	Axial crack transected weld.
SC0072 (CPV-12)	2.7		134	None	None
SC0073 (CPV-12)	2.4		92	None	None
SC0074 (CPV-12	3.1		280	None	None
SC0075 (CPV-12)	2.5		84	None	None

[a]Angular location referenced to the weld start to 0 deg.

A. CPV-1

Capsule SC0011, loaded with a hot-pressed urania pellet, was impacted against a 25.4-mm-thick structural steel plate at 55.0 ±1.0 m/s and 1092°C. The iridium hardware used for this capsule was Z-batch material produced for the Galileo and Ulysses missions. The clad impact face was centered approximately 60 deg from the weld start. The clad appeared to be breached by three cracks: a centerline weld crack centered at approximately 330 deg and two smaller transverse cracks on the cup radii at the edges of the impact face (Fig. 2). A small amount of urania (0.0415 g) was observed in the tantalum containment vessel. There was no detectable deformation of the steel target. The results of particle size analysis of the released and retained fuel are given in Table VII.

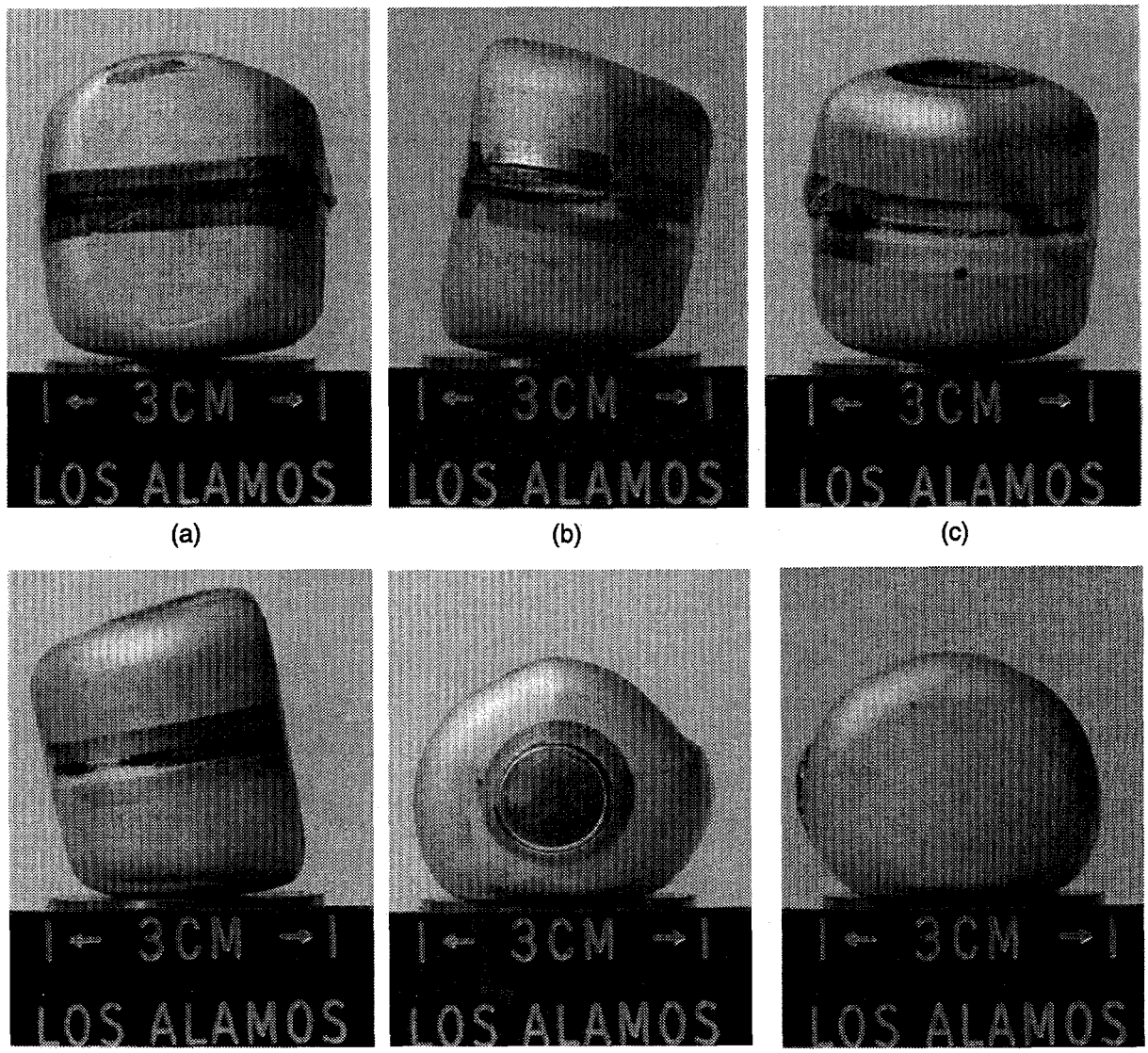

Figure 2. Capsule SC0011 appeared to be breached by a centerline weld crack at approximately 330 deg and two small cracks on the cup radii on the impact face. (a) impact face, (b) profile, (c) trailing face, (d) opposite profile, (e) vent end, (f) blind end, (g) fuel fragmentation. (NMT-9 Negs 92-58, 92-61, 92-60, 92-59, 92-56, 92-57, 92-62)

The body of the centerline weld crack was approximately 25.4 mm long and had a maximum width of approximately 1.27 mm at 300 deg from the weld start. At 270 deg from the weld start, the crack propagated upward into the vent cup at a 45 deg angle; this section of the crack had a length of approximately 6.35 mm. It appeared that this crack was caused by differential displacement of a large simulant fuel fragment, which creased the vent cup wall at 270 deg. The edge of this fragment was sharp enough to pierce the underlying weld shield so that the breached shield was clearly visible inside the weld crack. Examination of the microstructure confirmed that the breach did not result from a weld defect. The weld microstructure was generally fine-grained, and the breaching crack did not occur along the weld centerline (Fig. 3).

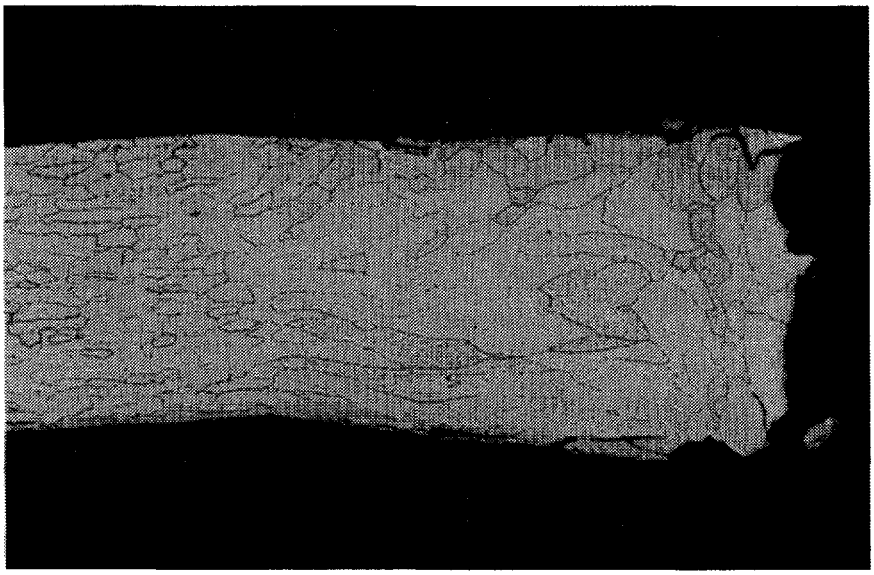

(a)

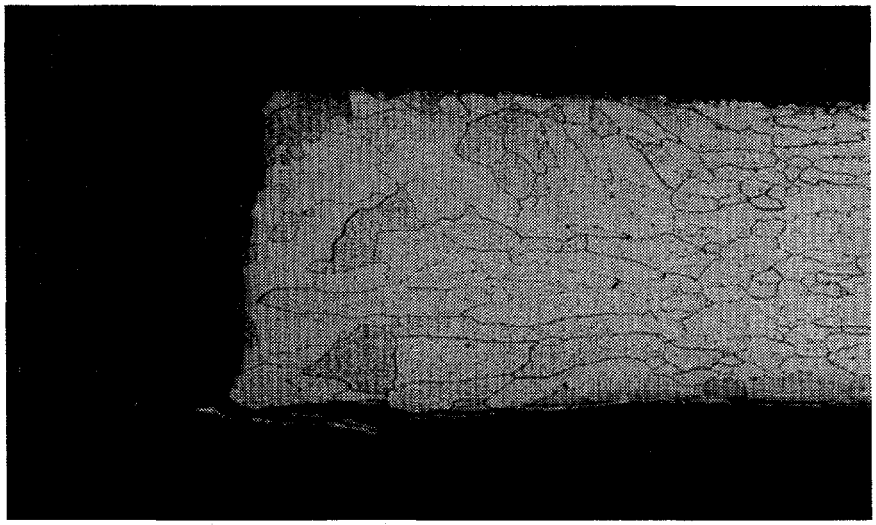

(b)

Figure 3. The weld breach crack was fine-grained and did not occur along the weld centerline. (a) and (b), both etched and at 50× magnification. (NMT-9 Negs 93-69 and 93-70)

The hairline cracks on the cup radii at the edges of the impact face appeared similar to the cracks observed in other capsules impacted at this velocity. The transverse crack in the shield cup was approximately 7.6 mm long, and the crack on the vent cup radius had a length of approximately 6.35 mm. Two small, nonpenetrating, axial cracks, approximately 5.0 mm long, were also observed on the edges of the impact face at the clad equator.

Another feature revealed by metallographic examination was the presence of a large offset between the vent and shield cup walls at a radial location of 144 deg from the weld start (Fig. 4). Although the outer surfaces of the cups were flush, the inner surfaces were offset by 0.125 mm. In this cross section, the apparent thicknesses of the vent and weld shield cups at the weld were 0.845 mm and 0.720 mm. The current Y-12/MMES specification for maximum wall thickness in this region is 0.73 mm. Interestingly, the anamalous wall thickness did not appear to have prevented full weld penetration or to have adversely affected the resulting weld microstructure.

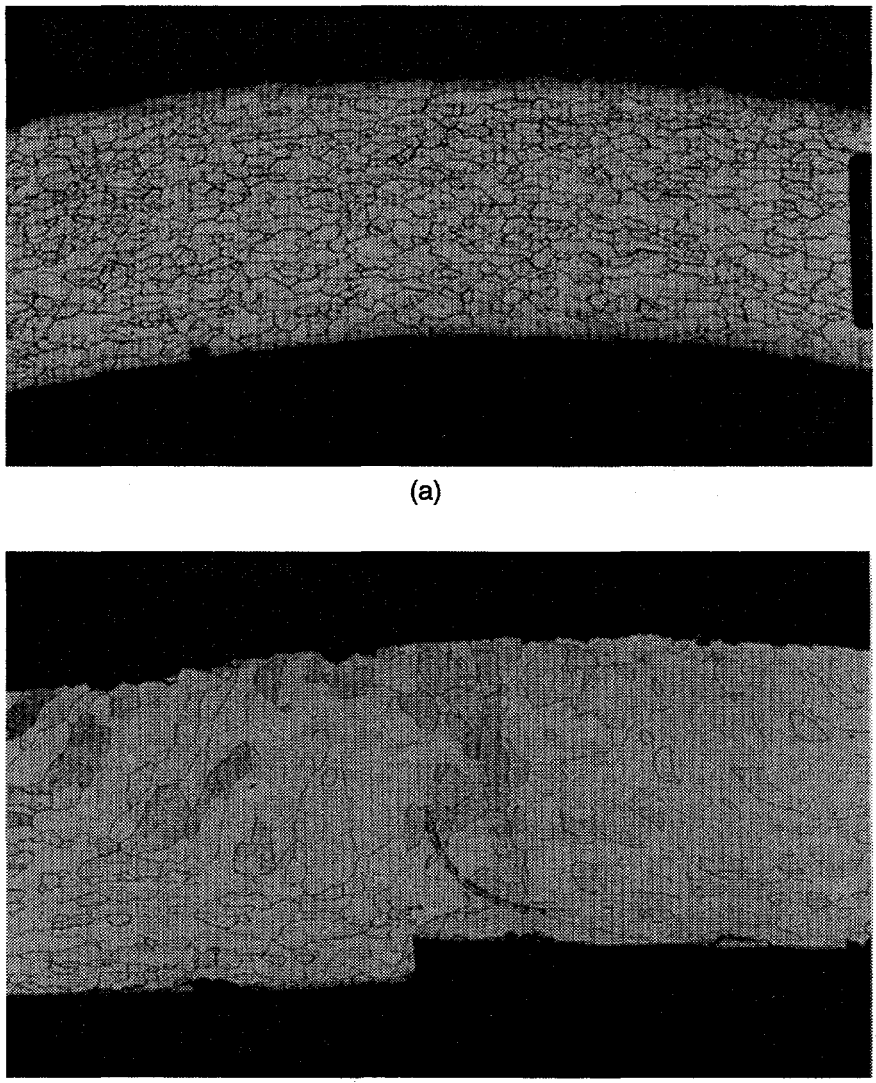

Figure 4. Large offset between the vent and shield cup walls at 144 deg from weld start; etched, at 50× magnification. (NMT-9 Neg 93-65)

Metallographic examination of a transverse section removed from the shield cup revealed a microstructure that was more refined than is typically observed in the cup walls (Fig. 5). The average grain size in this section was approximately half the size usually seen. Average vent and shield cup wall grain sizes are listed in Table X.

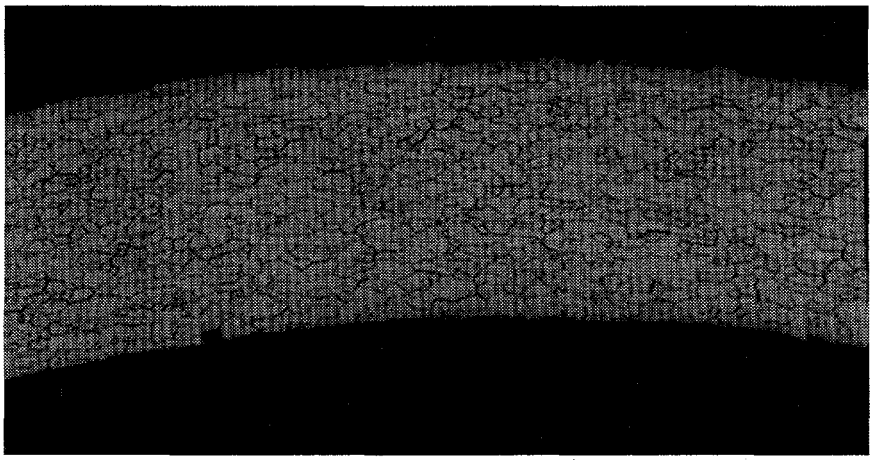

Figure 5. Unusual fine-grained microstructure; etched, at 50× magnification. (NMT-9 Neg 93-71)

B. CPV-2

Capsule SC0008, loaded with a hot-pressed urania pellet, was impacted against a 25.4-mm-thick structural steel plate at 55.0 ±1.0 m/s and 1090°C. The iridium harware used for this capsule was designated as "prime" and was from the D2 batch. The clad impact face was centered approximately 120 deg from the weld start. Post-impact examination revealed that although the capsule had two small transverse cracks on the cup radii at the edges of the impact face, no urania was released into the tantalum can (Fig. 6). Alpha counting of the swipes taken on the clad exterior and interior of the tantalum can confirmed that no fuel simulant had been released. There was no detectable deformation of the steel target. The capsule strains are listed in Table VI. The results of particle size analysis of the retained fuel is given in Table VII.

The hairline cracks on the cup radii at the edges of the impact face appeared to be similar to the cracks observed in other capsules impacted at this velocity. The transverse crack in the shield cup was approximately 6.0 mm and the crack on the vent cup radius was approximately 8.0 mm long. Metallographic examination confirmed that these cracks penetrated the capsule wall. Because the iridium microstructure in the vicinity of both cracks was exemplary and because the cracks appeared similar to the radius cracks on other capsules impacted at this velocity, it is unlikely that they were related to any materials defects.

Examination of the overlap region of the girth weld, at a weld location of 15 deg (weld start was at 0 deg), revealed that the weld shield had been completely incorporated into the weld pool (Fig. 7). The chill caused by the weld-shield fusion produced a weld microstructure that consisted primarily of thin columnar grains oriented normal to the cup walls. This metallographic evidence confirmed that the large UT reflector located between 0 and 30 deg was not a defect, (e.g., a weld crack) but was caused by the geometry of the weld-shield fusion.

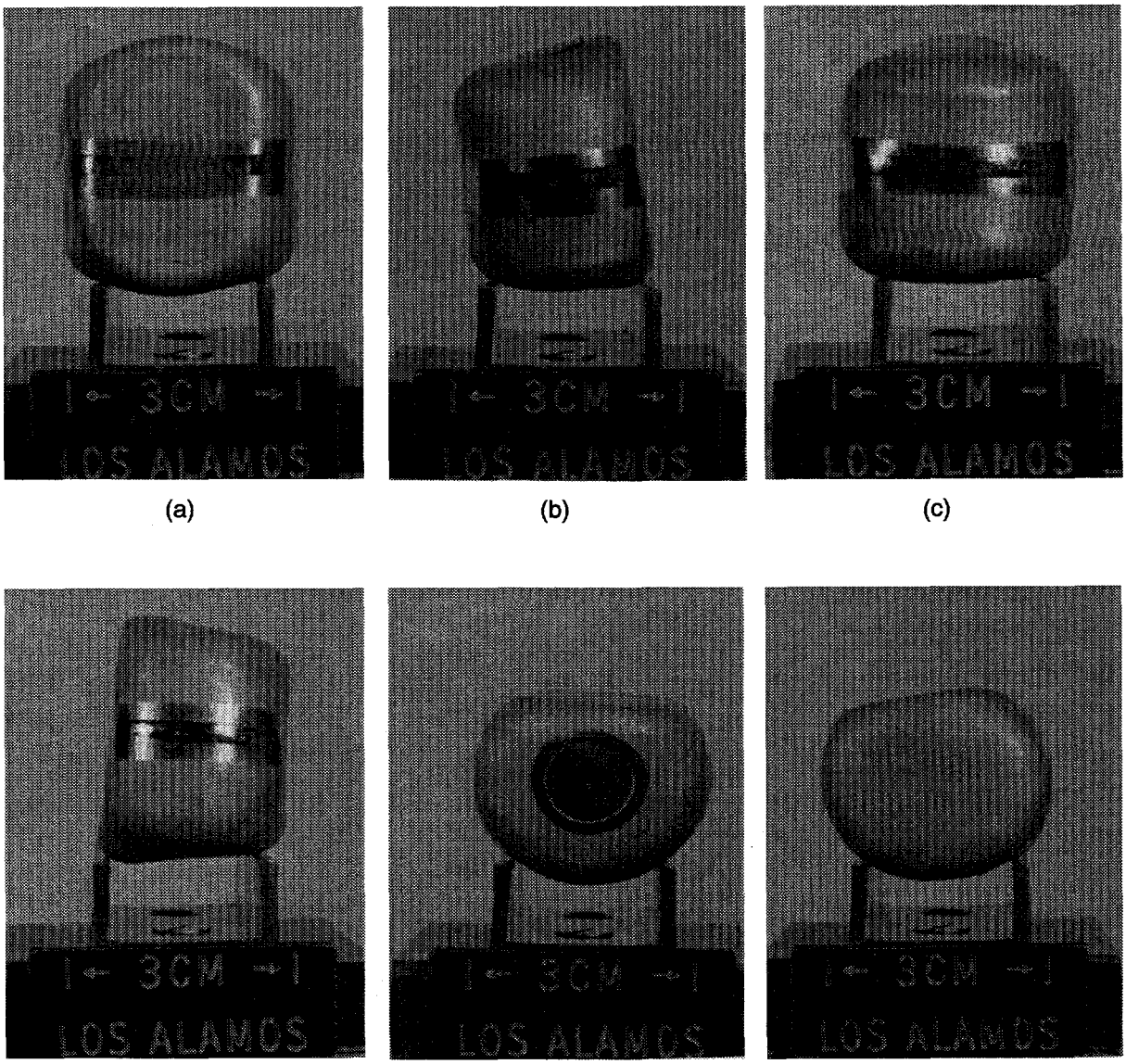

Figure 6. Two small cracks were observed on the impact face of capsule SC0008. (a) impact face, (b) profile, (c) trailing face, (d) opposite profile, (e) vent end, (f) blind end, (g) fuel fragmentation. (NMT-9 Negs 931-16, 931-19, 931-18, 931-17, 931-14, 931-15, 93-98)

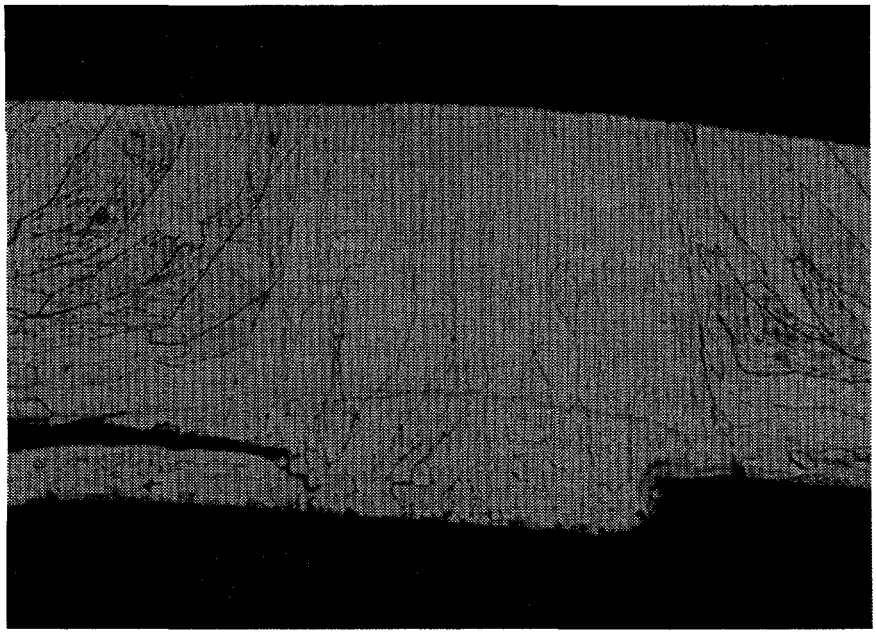

Figure 7. Weld-weld shield fusion locate at 15 from weld start; etched, at 50× magnification. (NMT-9 Neg 931-11)

Metallographic examination of a transverse section removed from the vent cup revealed an unusual microstructure (Fig. 8). Very fine grains were observed in the wall centerline, and isolated large grains were observed on both the interior and exterior of the wall. Average vent and shield cup wall grain sizes are listed in Table X.

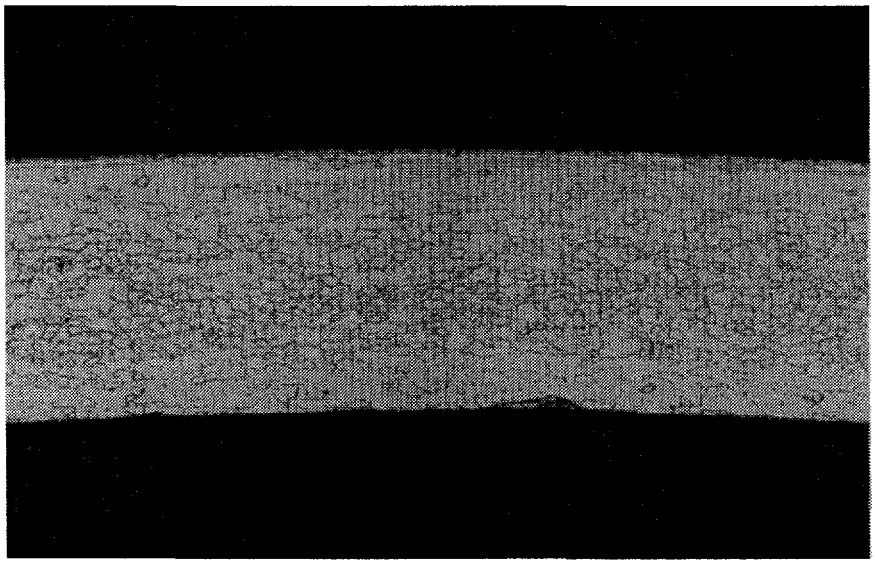

Figure 8. Unusual microstructure; etched, at 50× magnification. (NMT-9 Neg 931-10)

C. CPV-3

Capsule SC0004, loaded with a cold-pressed and sintered urania pellet, was impacted against a 25.4-mm-thick structural steel plate at 55.0 ± 0.1 m/s and 1090°C. The iridium hardware used in this capsule was designated as "prime" and was from the D2 batch. The clad impact face was centered at approximately 120 deg from the weld start (Fig. 9). Two small cracks were on the vent cup radius at the edge of the impact face. No urania was observed in the tantalum containment vessel. Alpha counting of swipes taken on the clad exterior and interior of the tantalum can confirmed that no fuel had been released. There was no detectable deformation of the steel target. The capsule strains are given in Table VI. The particle size analysis of the retained fuel is given in Table VII.

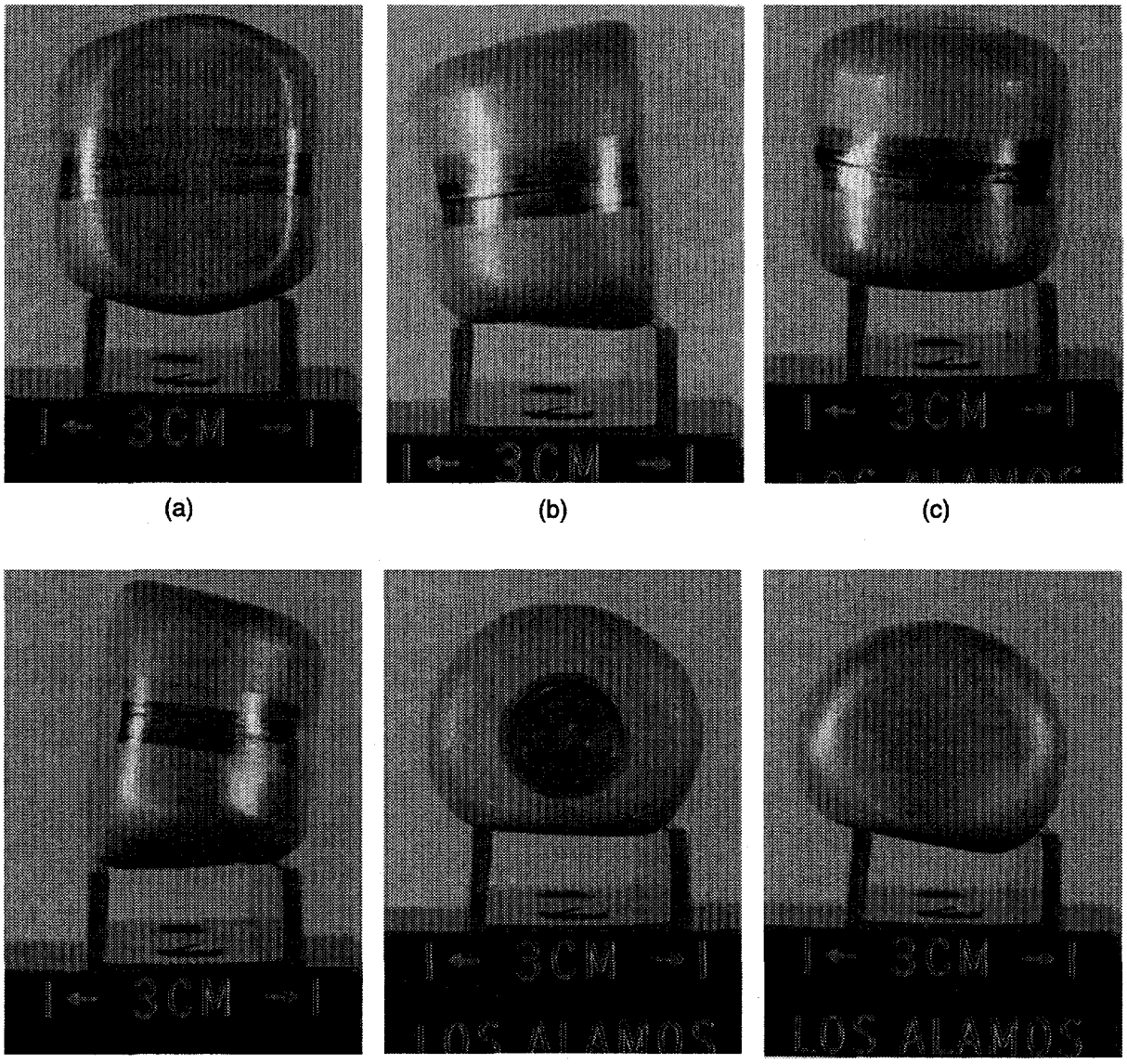

Figure 9. Two small cracks were observed on the impact face radius of capsule SC0004. (a) impact face, (b) profile, (c) trailing face, (d) opposite profile, (e) vent end, (f) blind end, (g) fuel fragmentation. (NMT-9 Negs 93-94, 93-97, 93-96, 93-95, 93-93, 93-92, 931-21)

The hairline cracks on the vent cup radius measured approximately 4.5 mm in length. The radius cracks appear similar to the cracks observed in other capsules impacted at this velocity. Metallographic examination of these cracks revealed that they penetrated the capsule wall and were intergranular. The microstructure of these cracks was similar to that of cracks observed on the impact faces of other CPV capsules.

Examination of the defueled crack revealed a number of internal cracks that were not visible on the clad exterior. A short 5.0 mm transverse crack was present on the impact face of the shield cup radius. Metallographic examination revealed the intergranular nature of this crack that nearly penetrated the clad wall. Three small axial cracks (up to 2.0 mm) extended from the vent cup to the weld centerline. The axial cracks were located at the edges of the impact face, with two cracks on one side and the remaining crack on the opposite side. All of these cracks appeared to have originated at or near the weld centerline and then propagated along grain boundaries into the vent or weld shield cups. Metallographic examination of these cracks revealed that the single crack visible in the polished section was exclusively intergranular and extended through 85% of the weld thickness. Because no significant reflectors were detected during a pre-impact UT examination of the weld, it is apparent that this crack resulted from a mechanical interaction with the fragmenting fuel pellet. Average vent and shield cup wall grain sizes are listed in Table X.

D. CPV-4

Capsule SC0020, loaded with a cold-pressed urania pellet, was impacted against a 25.4-mm-thick structural steel plate at 55.25 ± 0.1 m/s and 1090°C. The iridium hardware used in this clad was obtained from Westinghouse Savannah River Company and was X- and YR-batch material produced for the Galileo and Ulysses missions. The clad impact face was centered at approximately 0 deg, weld start (Fig. 10). The clad was breached at approximately 120 deg by an axial crack that extended from the shield cup, through the weld, and into the vent cup. Smaller axial cracks also occurred at approximately 170, 180, and 225 deg. At approximately 180 deg, a network of hairline, generally axial, cracks were visible on the cup radii at the edges of the vent cup radius. Small transverse cracks were visible on the cup radii at the edges of the impact face. A small amount of urania (0.103 g) was released into the tantalum containment vessel. The capsule strains are listed in Table VI. The particle size analysis results are given in Table VIII.

The axial breach at 120 deg had a length of approximately 10.4 mm and a maximum width of approximately 0.65 mm. Examination of the opened capsule revealed that the axial breach matched the differential displacement of a large urania fragment. Microscopic examination of the widest section of the crack, just below the weld in the weld shield cup, revealed that it was exclusively intergranular (Fig. 11). There was no evidence to suggest that the breaching crack resulted from any defects or anomalies in either the weld shield cup or the girth weld.

The axial weld cracks at 170, 180, and 225 deg were all contained within the weld metal. The cracks at 170 and 180 deg were approximately 1.3 mm long, and the crack at 225 deg had a length of approximately 2.3 mm. The network of hairline cracks at 180 deg had an approximate length of 10.0 mm and appeared to be related to severe localized deformation caused by the displacement of a sharp fuel fragment. Metallographic examination of these cracks revealed that they were all intergranular and occurred in regions of fine-grained microstructure.

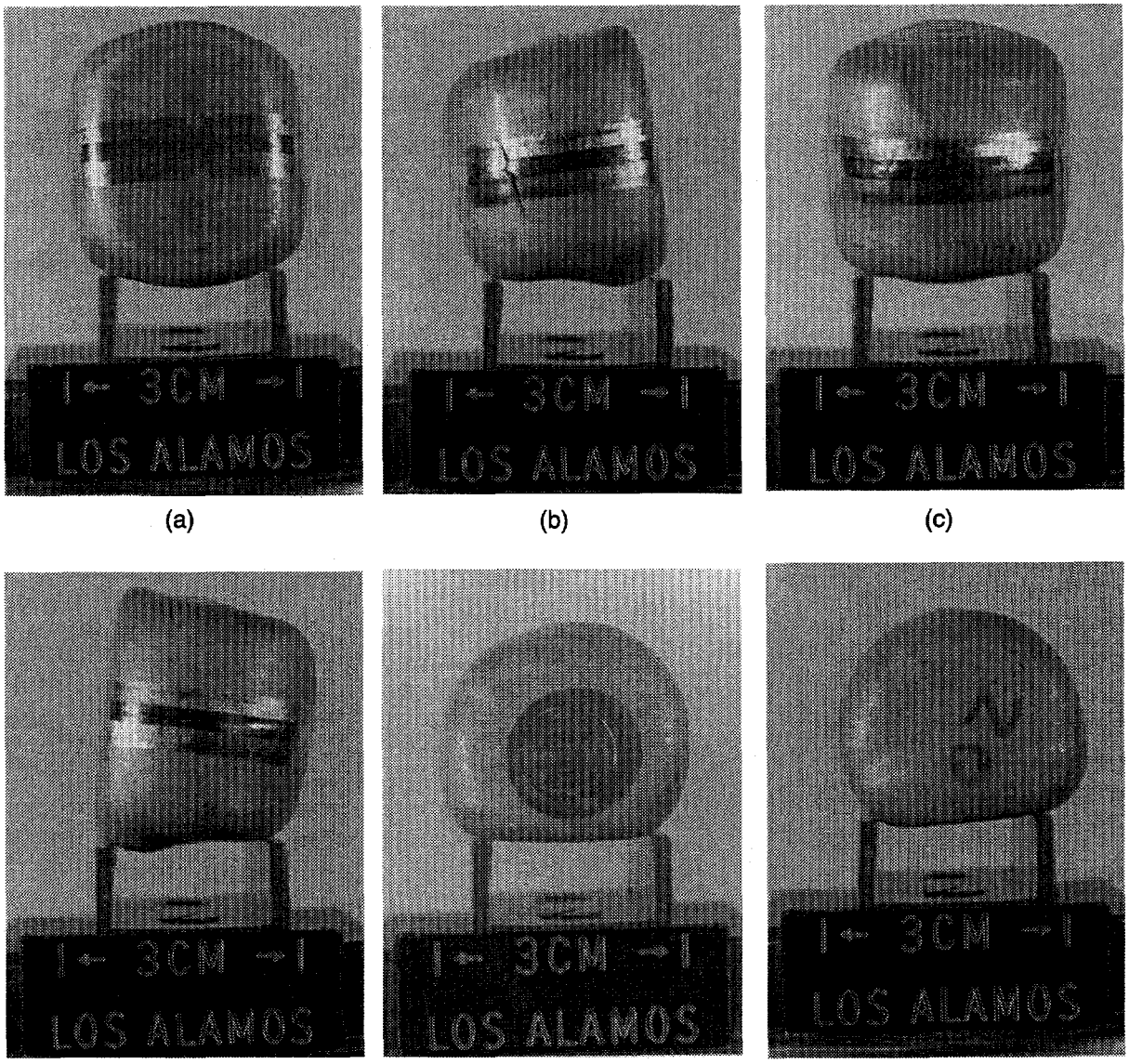

Figure 10. Capsule SC0020 was breached by an axial crack at approximately 120 deg. (a) impact face, (b) profile, (c) trailing face, (d) opposite profile, (e) vent end, (f) blind end, (g) fuel fragmentation. (NMT-9 Negs 93-85, 93-88, 93-87, 93-86, 93-84, 93-83, 94-15)

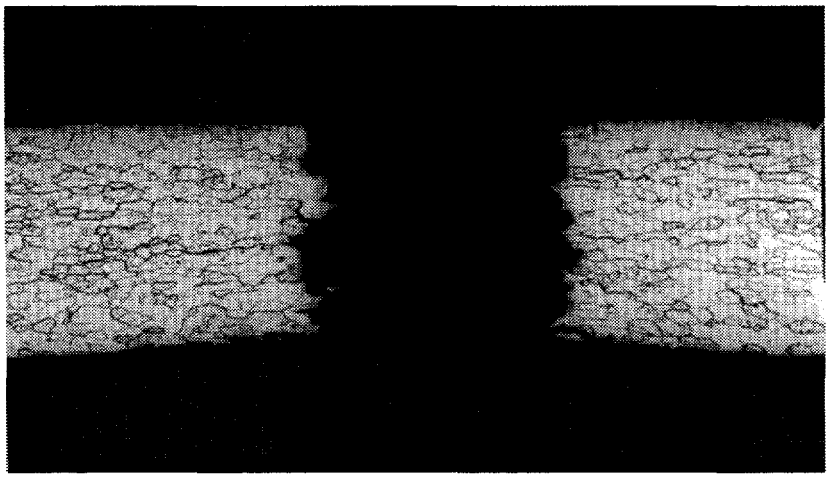

Figure 11. The axial breaching crack was exclusively intergranular; etched, at 50× magnification. (NMT-9 Neg 941-43)

The transverse cracks on the impact face of the vent and shield cup radii appeared similar to cracks observed in other capsules impacted at this velocity. The crack in the vent cup radius was approximate 11.0 mm long, and the crack on the shield cup radius had an approximately length of 5.5 mm. These cracks were determined to be intergranular and in fine-grained regions with metallographic examination. Average vent and shield cup wall grain sizes are listed in Table X.

E. CPV-5

Capsule SC0017, loaded with a cold-pressed urania pellet, was impacted against a 25.4-mm-thick structural steel plate at 55.3 ±0.1 m/s and 1090°C. The iridium hardware used in this clad was designated as "prime" and was from the D2 batch. The clad impact face was centered at approximately 120 deg from the weld start (Fig. 12). The capsule was breached by a transverse crack on the impact face of the vent cup radius and by an axial crack on the edge of the vent cup impact face at approximately 90 deg. A number of small axial cracks were also observed on the edge of the shield cup impact face at 150 deg. A very small amount of urania, which could not be collected for particle size analysis, was released into the tantalum containment vessel. There was no detectable deformation of the steel target. The capsule strains are listed in Table VI. The particle size analysis results are given in Table VIII.

The transverse crack on the vent cup radius had a total length of approximately 18.0 mm. However, only 6.5 mm of the crack had a measurable width. The maximum crack width was approximately 0.9 mm. The crack was exclusively intergranular and appeared to be similar to the cup radii cracks observed on the capsule impact face. The small axial cracks (each less than 2.5 mm) that were present on the impact face of the shield cup and weld were nonpenetrating (Fig. 13).

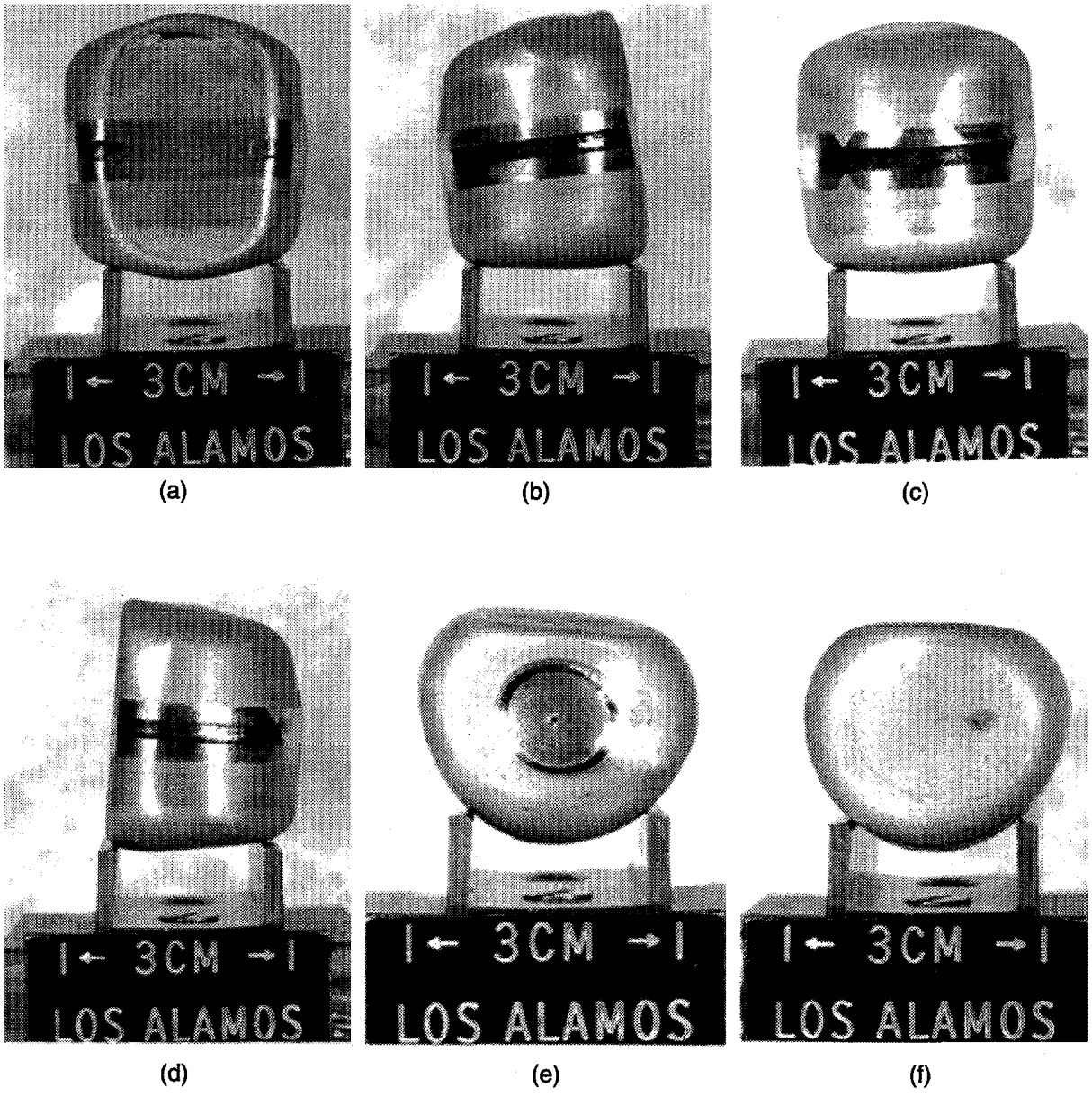

Figure 12. Capsule SC0017 was breached by a transverse and an axial crack on the impact face.(a) impact face, (b) profile, (c) trailing face, (d) opposite profile, (e) vent end, (f) blind end. (NMT-9 Negs 931-22, 931-25, 931-24, 931-23, 931-26, 931-28)

The axial crack at 90 deg, on the edge of the impact face, had an approximate length of 12.5 mm and a negligible width. Although the bulk of the crack was located in the vent cup and may have been related to the crack on the vent cup radius, the lower portion of the crack traversed the weld and terminated in the weld shield cup (Fig. 14). The radial displacement of the crack ends suggests that the failure resulted from differential displacement of a large fuel fragment.

The microstructures of the weld in the single-pass and overlap regions were typical and did not reveal any anomalies. Average vent and shield cup wall grain sizes are listed in Table X.

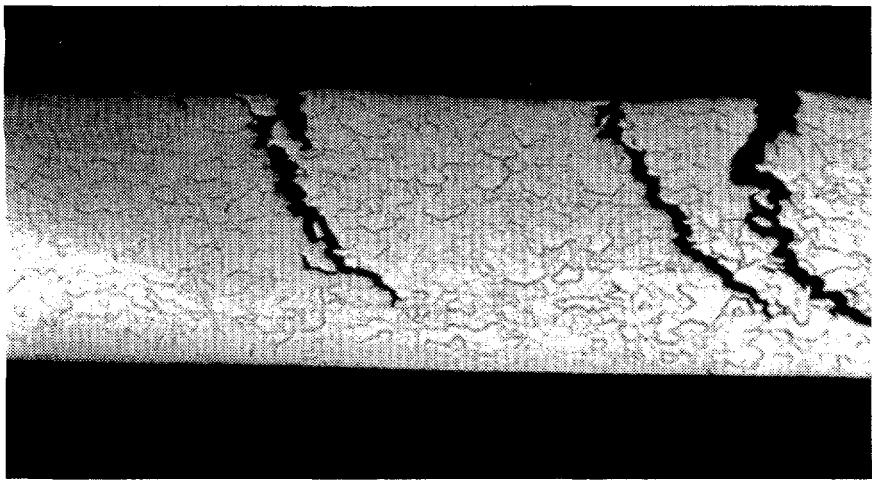

Figure 13. Nonpenetrating impact face axial cracks; etched, at 50× magnification. (NMT-9 Neg 942-17)

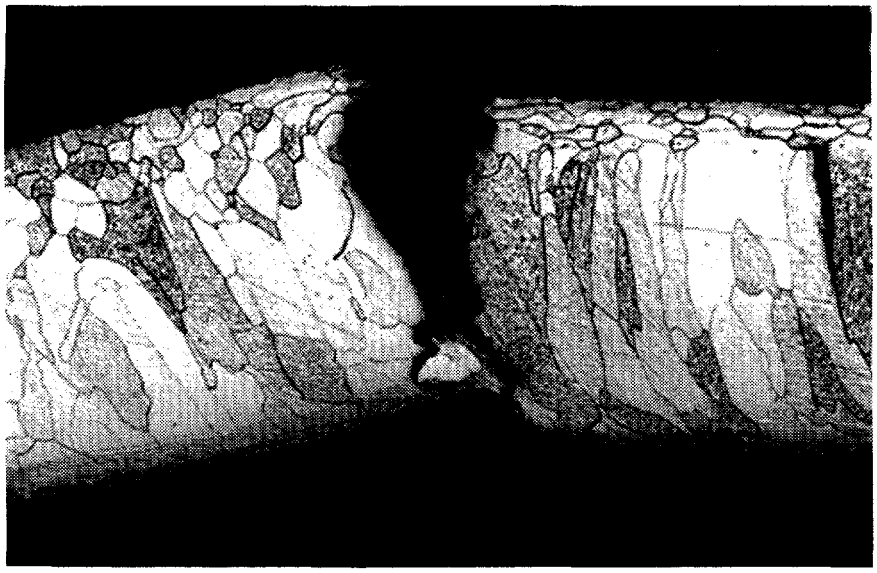

Figure 14. Breaching axial impact face crack; etched, at 50¥ magnification. (NMT-9 Neg 942-20)

F. CPV-6

Capsule SC0018, loaded with a cold-pressed and sintered pellet, was impacted against a 25.4-mm-thick structural steel plate at 55.0 ± 0.1 m/s and 1090°C. The iridium hardware used in this clad was designated as "prime" and was from the CR3 batch. The clad impact face was centered at approximately 30 deg from the weld start (Fig. 15). A network of hair-line axial cracks was observed on the edge of the impact face. No urania was released into the tantalum containment vessel. There was no detectable deformation of the steel target. The capsule strains are listed in Table VI. The particle size analysis results are given in Table VIII.

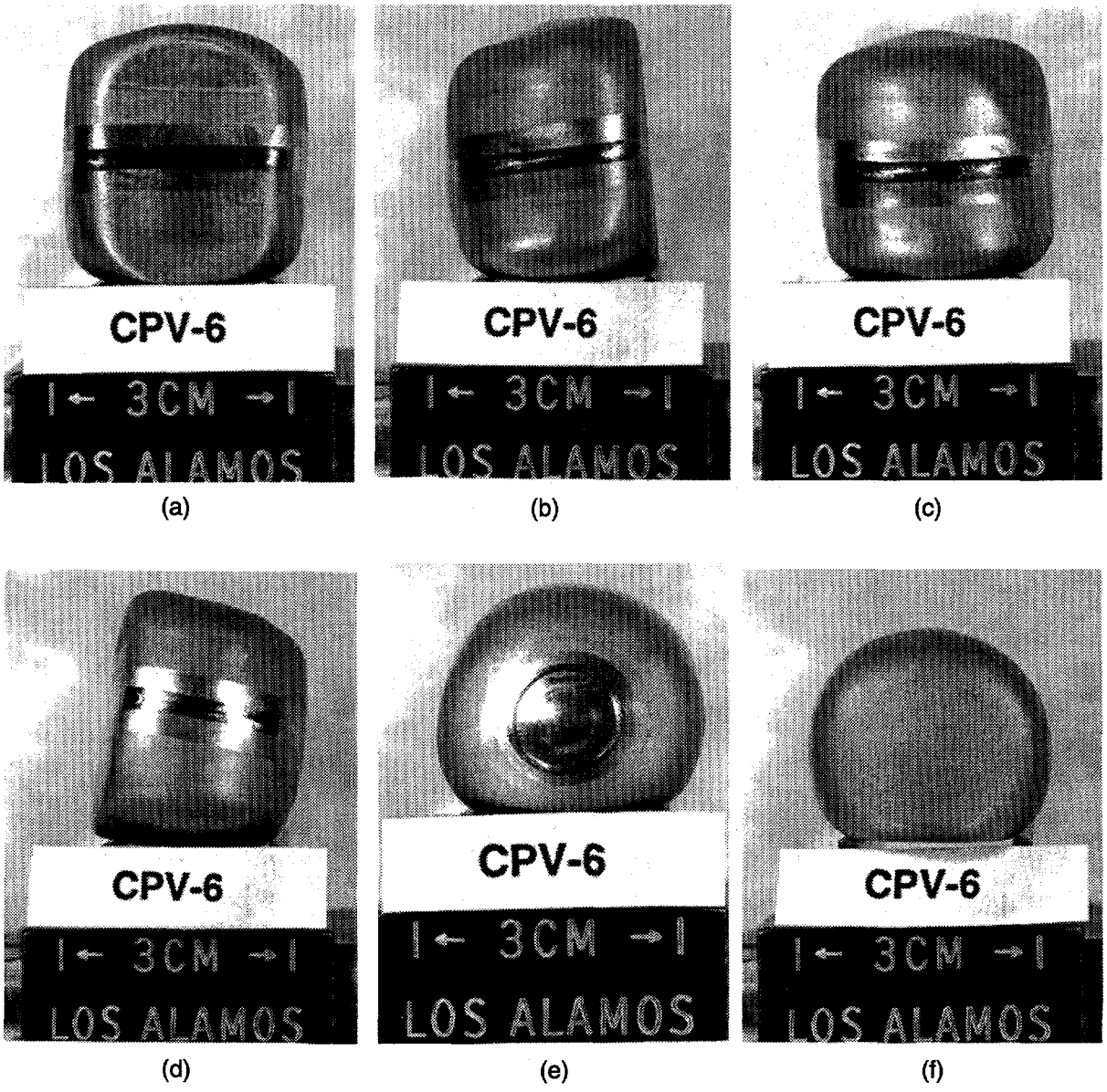

Figure 15. A network of hairline axial cracks were observed on the edge of the impact face.(a) impact face, (b) profile, (c) trailing face, (d) opposite profile, (e) vent end, (f) blind end. (NMT-9 Negs 931-31, 931-32, 931-33, 931-34, 931-35, 931-36)

The network of hairline axial cracks was located at the edge of the impact face at approximately 10 deg from the weld start. The largest portion of the crack network was located in the weld shield cup, but some cracks extended through the weld to the grit-blast line on the vent cup. The crack network had an overall length of approximately 12.5 mm. Metallographic examination of the cracks revealed a breaching crack in the weld area (Fig. 16). This crack had a maximum width of approximately 0.18 mm. No other breaching cracks were observed and all of the cracks were intergranular in fine-grained microstructure.

The microstructures of the weld in the single-pass and overlap regions were typical and did not reveal any anomalies. Average vent and shield cup wall grain sizes are listed in Table X.

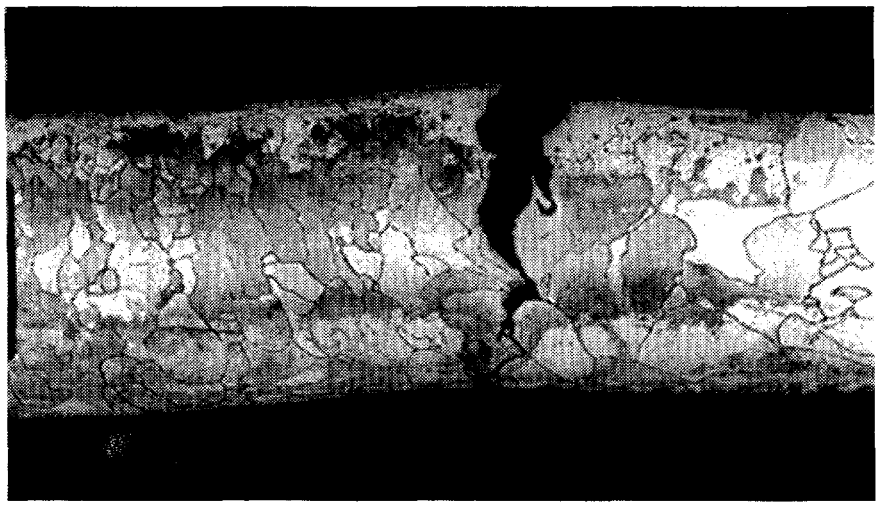

Figure 16. Breaching crack observed in network of hairline cracks in weld area; etched, at 50× magnification. (NMT-9 Neg 943-80)

G. CPV-7

Capsule SC0019, loaded with a cold-pressed and sintered pellet, was impacted against a 25.4-mm-thick structural steel plate at 55.3 ± 0.1 m/s and 1090°C. The iridium hardware used for this capsule was X- and YR-batch material produced for the Galileo and Ulysses missions. The clad impact face was centered at approximately 150 deg from the weld start (Fig. 17). No cracks were visible on the impact face of the capsule. The trailing face was breached by a centerline weld failure that extended from approximately 300 to 45 deg from the weld start and by a small axial crack in the weld shield cup at 270 deg. No urania was released into the tantalum containment vessel. The capsule strains are listed in Table VI. The particle size analysis results are given in Table VIII.

The centerline weld failure was approximately 22.5 mm long and had a maximum width of 0.64 mm. The weld shield was relatively intact and remained in position behind the weld crack. The weld failure appeared to be related to the anomalous displacement of fuel fragments contained within the vent and weld shield cups. The maximum displacement between the two cup sections was 1.63 mm.

At the termination of the weld failure (45 deg), a secondary crack extended into the weld shield cup. This crack was oriented at approximately 45 deg from the weld and had a length of approximately 5.1 mm. Over a major portion of the crack length, the underlying weld shield had been penetrated by what appeared to be a sharp urania fragment. Because the urania fragment was visible on the other side of the crack, it is unclear why no urania fines were released into the containment vessel.

The hairline axial crack at 270 deg extended from the weld shield cup to the weld centerline. The crack had a length of approximately 2.5 mm. It did not appear that this crack was related to the differential displacement of a urania fragment.

Several hairline axial cracks were also observed on the interior surface of the clad. The largest of these was a breaching crack with a maximum width of approximately 16 μm. None of the other axial cracks breached the clad; penetration of the other cracks varied from 25% to 75% of the wall thickness. All of the cracks observed, including the centerline failure, were intergranular.

Examination of the single-pass and overlap weld regions revealed typical microstructure. Average vent and shield cup wall grain sizes are listed in Table X.

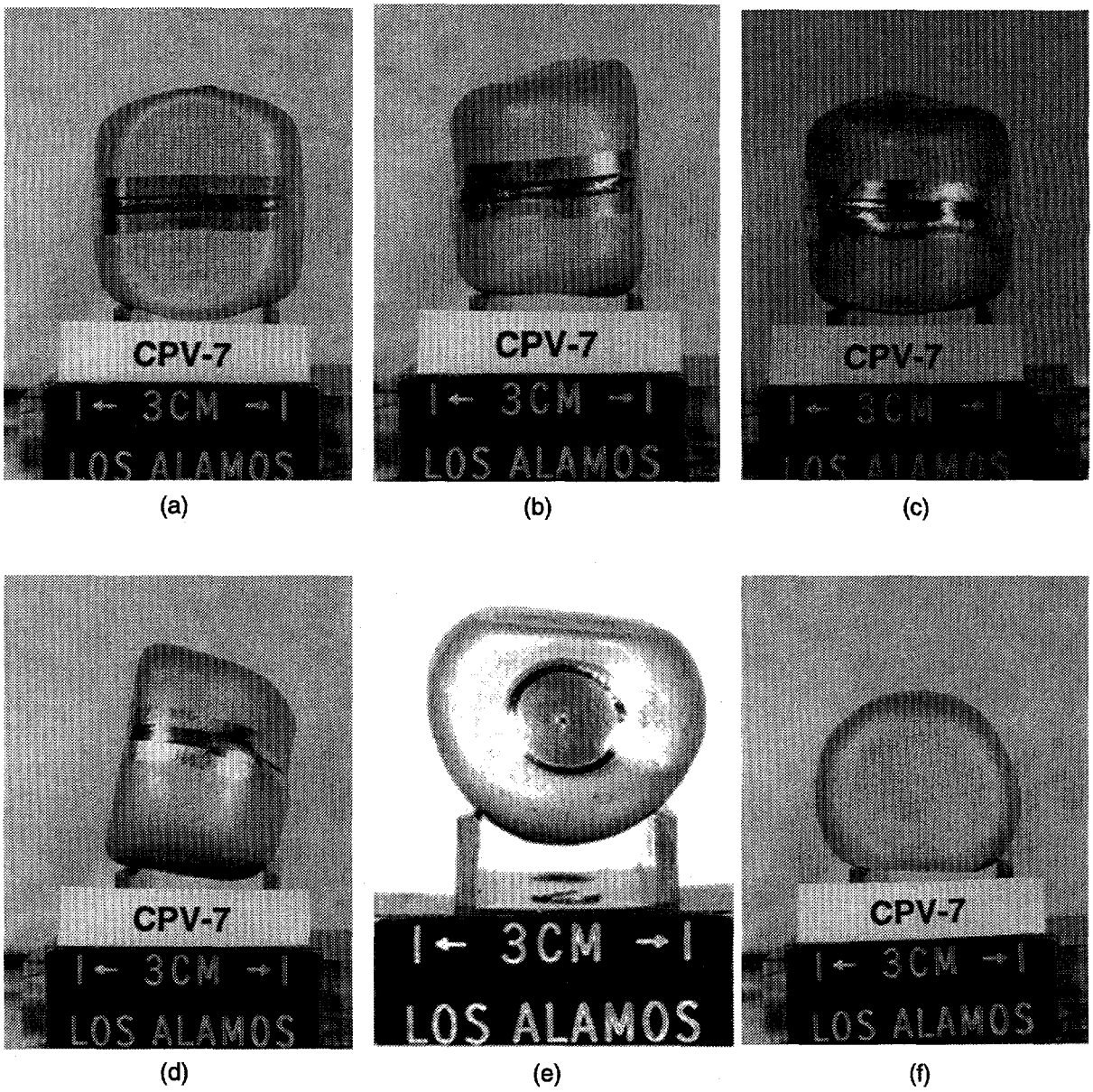

Figure 17. The trailing face of SC0019 was breached by a centerline weld failure. (a) impact face, (b) profile, (c) trailing face, (d) opposite profile, (e) vent end, (f) blind end. (NMT-9 Negs 931-37, 931-38, 931-39, 931-40, 931-41, 931-42)

H. CPV-8

Capsule SC0006, loaded with a cold-pressed and sintered urania pellet, was impacted against a 25.4-mm-thick structural steel plate at 55.3 ±0.4 m/s and 1090°C. The iridium hardware used for this capsule was designated as "prime" and was from the CR-3 batch. The impact face was centered at approximately 225 deg from the weld start (Fig. 18). Although a small transverse crack was observed on the impact face of the vent cup radius, no other cracks were observed on the clad. Ridges were observed on the trailing face of the capsule. No urania was observed in the tantalum containment vessel. There was no detectable deformation of the steel target. The capsule strains are listed in Table VI. The particle size analysis results are given in Table IX.

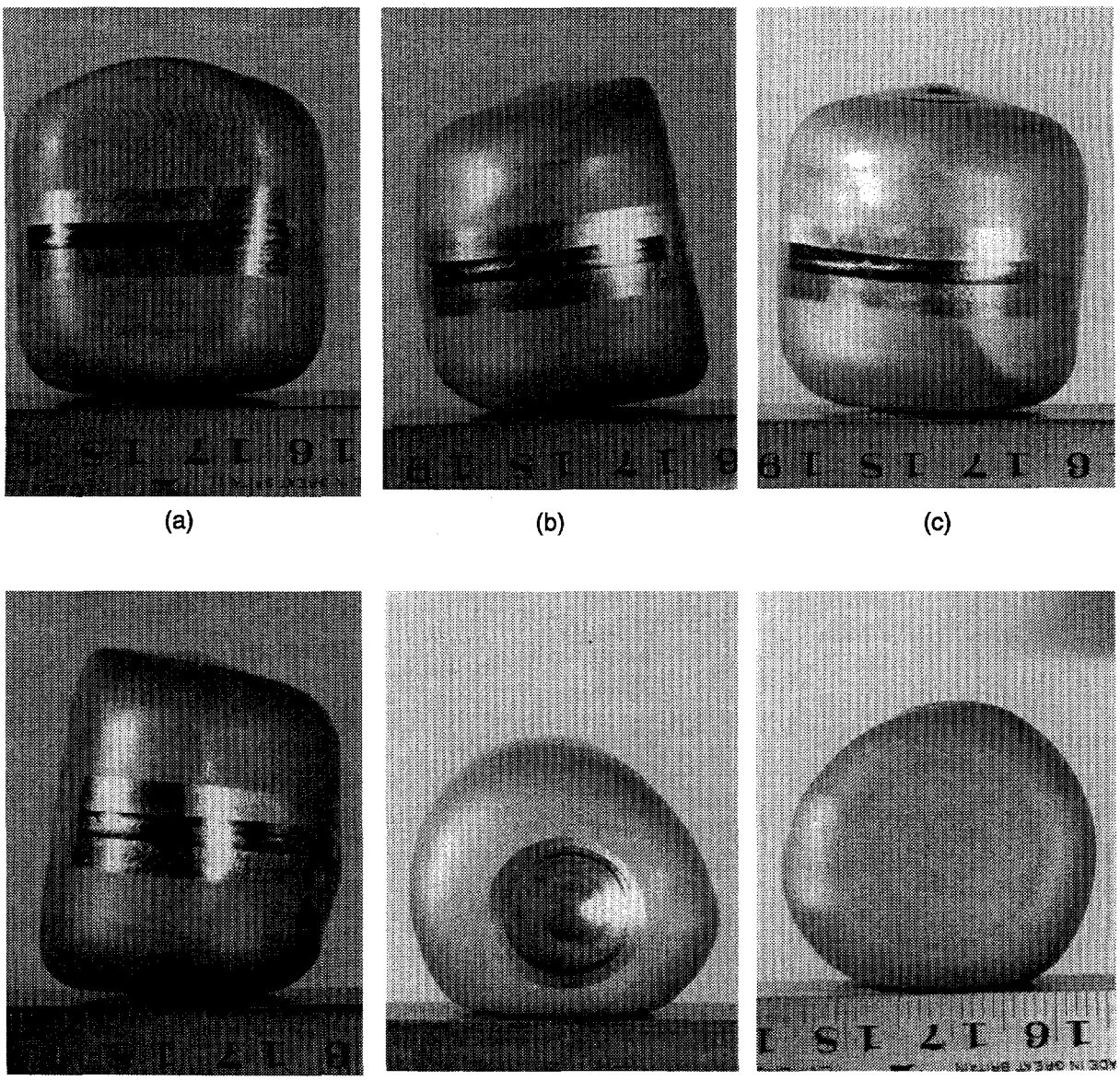

Figure 18. A small transverse crack was observed on the impact face vent cup radius of capsule SC0006. (a) impact face, (b) profile, (c) trailing face, (d) opposite profile, (e) vent end,(f) blind end, (g) fuel fragmentation. (NMT-9 Negs 941-62, 941-63, 941-61, 941-59, 941-60, 941-64, 941-65)

Metallographic examination of the impact face crack revealed a nonpenetrating intergranular failure with fine-grained microstructure (Fig. 19). Other similar nonpenetrating cracks were observed; all were intergranular. The cracks and the ridges observed on the trailing face of the capsule appear to have been caused by pellet fragment displacement.

Examination of the single-pass and overlap weld regions revealed typical microstructure. Average vent and shield cup wall grain sizes are listed in Table X.

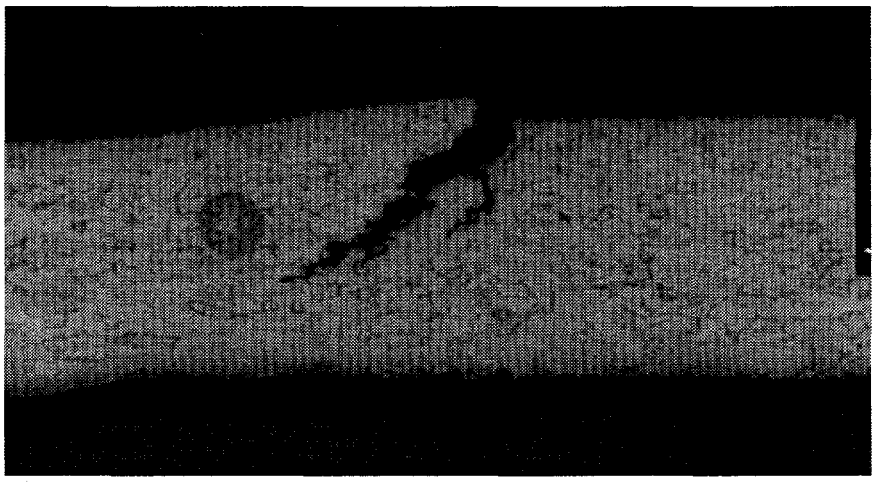

Figure 19. Nonpenetrating intergranular failure; etched, at 50× magnification. (NMT-9 Neg 945-7)

I. CPV-9

Capsule SC0015, loaded with a hot-pressed urania pellet, was impacted against a 25.4-mm-thick structural steel plate at 54.46 ± 0.04 m/s and 1090°C. The iridium hardware used for this capsule was designated as "prime" and was from the CR3 batch. The impact face was centered at approximately 120 deg from the weld start (Fig. 20). Two hairline transverse cracks were visible on the impact face of the cup radii. A small axial crack was located at approximately 210 deg on the vent cup. A very small amount of urania fines was detected in the tantalum containment vessel but could not be collected for particle size analysis. There was no detectable deformation of the steel target. The capsule strains are listed in Table VI. The particle size analysis results are given in Table IX.

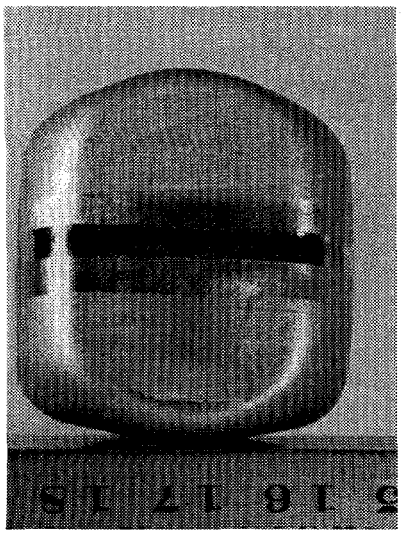

(a)

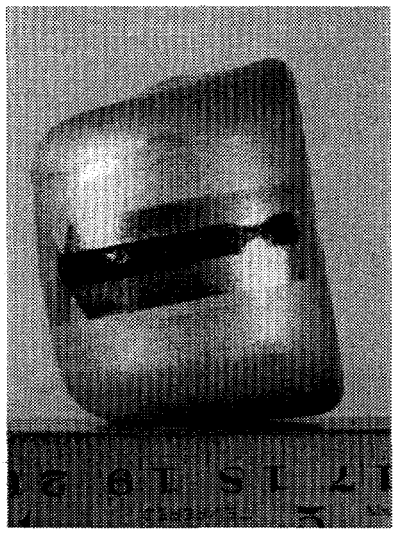

(b)

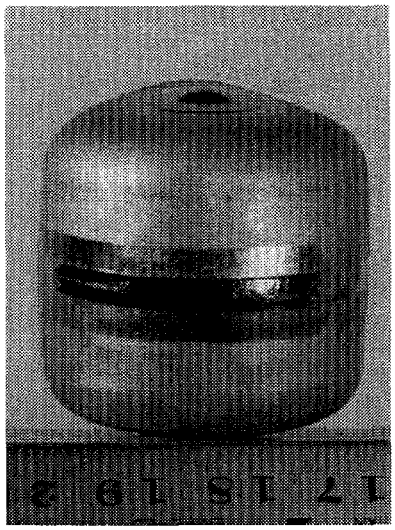

(c)

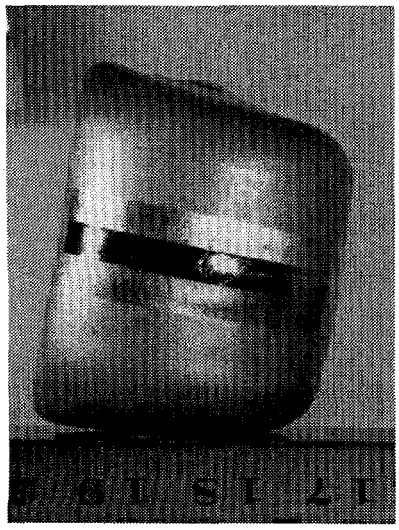

(d)

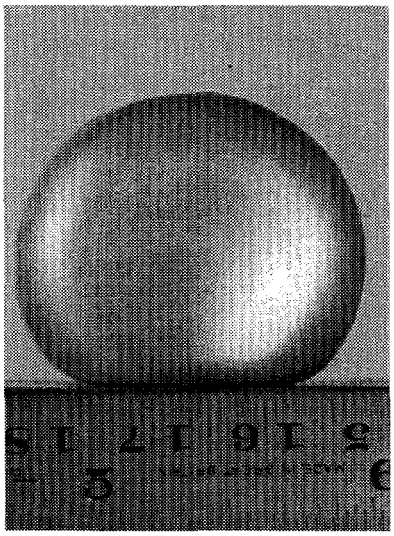

(e)

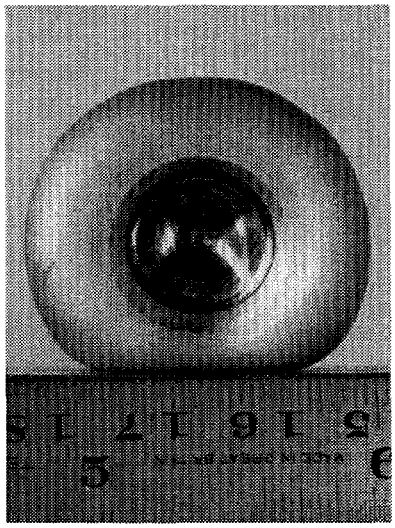

(f)

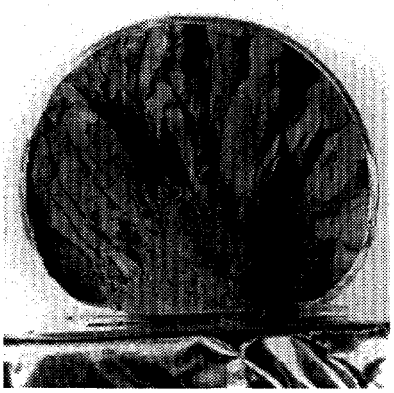

(g)

Figure 20. Capsule SC0015 appeared to be breached by two transverse impact face cracks and a small axial crack at approximately 210 deg. (a) impact face, (b) profile, (c) trailing face, (d) opposite profile, (e) vent end, (f) blind end, (g) fuel fragmentation. (NMT-9 Negs 941-70, 941-66, 941-71, 941-67, 941-68, 941-69, 941-72)

The transverse crack on the vent cup in the impact face had a length of approximately 7.9 mm, and the crack on the shield cup in the impact face was approximately 9.6 mm. Metallographic examination of these cracks revealed that the vent cup crack was a breaching, intergranular crack (Fig. 21). The shield cup crack was nonpenetrating but also intergranular. The hairline axial crack at 210 deg measured approximately 2.7 mm. This crack started just above the weld centerline and extended into the vent cup. This crack was also intergranular.

Examination of the weld overlap area revealed a slight bulge (Fig. 22). The minimum width of the capsule wall in this area was 0.57 mm. The maximum wall width measured approximately 0.75 mm. The microstructure in this area was somewhat coarse grained, however, the wall thinning that resulted from the weld bulge did not adversely affect the capsule's impact performance; no failures were observed in this region.

Examination of the single-pass weld regions revealed typical microstructure. Average vent and shield cup wall grain sizes are listed in Table X.

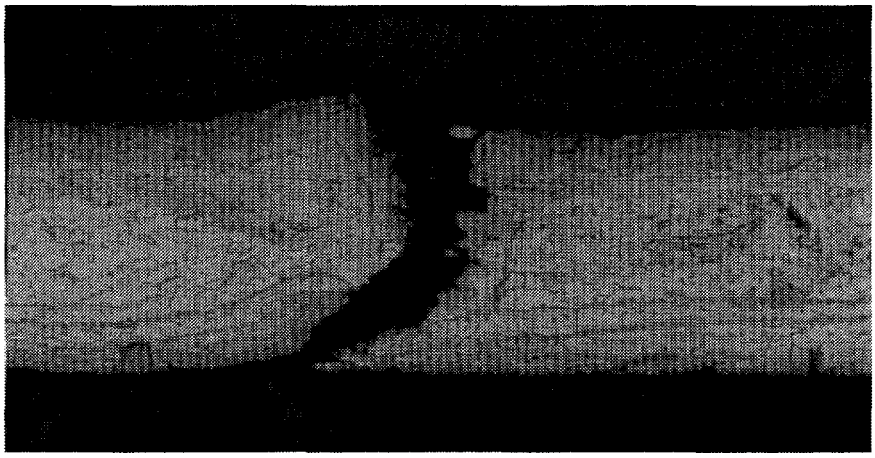

Figure 21. Axial vent cup crack; etched, at 50× magnification. (NMT-9 Neg 945-28)

Figure 22. Bulge in weld overlap area, etched, at 50× magnification. (NMT-9 Neg 945-16)

J. CPV-10

Capsule SC0009, loaded with a hot-pressed urania pellet, was impacted against a 25.4-mm-thick structural steel plate at 54.54 ± 0.04 m/s and 1090°C. The iridium hardware used for this capsule was designated as "prime" and was from the CR3 batch. The impact face was centered at approximately 90 deg from the weld start (Fig. 23). Two hairline transverse cracks were visible on the top and bottom edges of the impact face. A small axial crack that transected the weld was located at approximately 315 deg from the weld start. No urania was observed in the tantalum containment vessel. There was no detectable deformation of the steel target. The capsule strains are listed in Table VI. The particle size analysis results are given in Table IX.

The transverse crack on the impact face of the vent cup measured approximately 10.2 mm in length. The transverse crack on the shield cup impact face was approximately 6.6 mm long. Both cracks were intergranular and were similar to transverse radial impact face cracks observed in other simulant-fueled GPHS capsules impacted at these conditions.

The axial crack at 315 deg measured approximately 7.8 mm in length. This hairline crack, which was located on the trailing face and appeared to have been caused by pellet fragment displacement, was intergranular.

Examination of the single-pass and overlap weld regions revealed typical microstructure. Average vent and shield cup wall grain sizes are listed in Table X.

K. CPV-11

Capsule SC0016, loaded with a hot-pressed pellet, was impacted against a 25.4-mm-thick structural steel plate at 54.78 ± 0.08 m/s and 1090°C. The iridium hardware used for this capsule was X- and YR-batch material produced for the Galileo and Ulysses missions. Although the test was intended to be a side-on impact, the capsule apparently was released from the positioning cradle during transportation to the launcher facility. The capsule impacted on the end of the shield cup (Fig. 24). Surprisingly, the capsule deformation was relatively modest (Table VI). However, a relatively large hairline crack was observed on the impact face of the capsule. Two large axial cracks that transected the weld were observed approximately 270 deg from the weld start. No urania was observed in the tantalum containment vessel and there was no detectable deformation of the steel target. The capsule strains are listed in Table VI. The particle size analysis results are given in Table IX.

The hairline radial crack on the impact face measured approximately 18.7 mm in length. Metallographic examination of the crack showed it to be intergranular.

The axial cracks measured approximately 11.8 mm and 6.7 mm in length. The longest crack had a maximum width of approximately 1.4 mm located just above the weld centerline. The width of the smaller axial crack, located just below the weld in the shield cup, measured approximately 0.4 mm. The weld shield was intact between the clad and the pellet and probably prevented the release of any urania from the capsule. Examination of these cracks revealed intergranular failure with a small amount of radial displacement and wall thinning (Fig. 25). The lack of any other microstructural evidence suggests that the cracks were not caused by anything other than pellet fragmentation displacement.

Examination of the single-pass and weld overlap regions revealed typical microstructures. Average vent and shield cup wall grain sizes are listed in Table X.

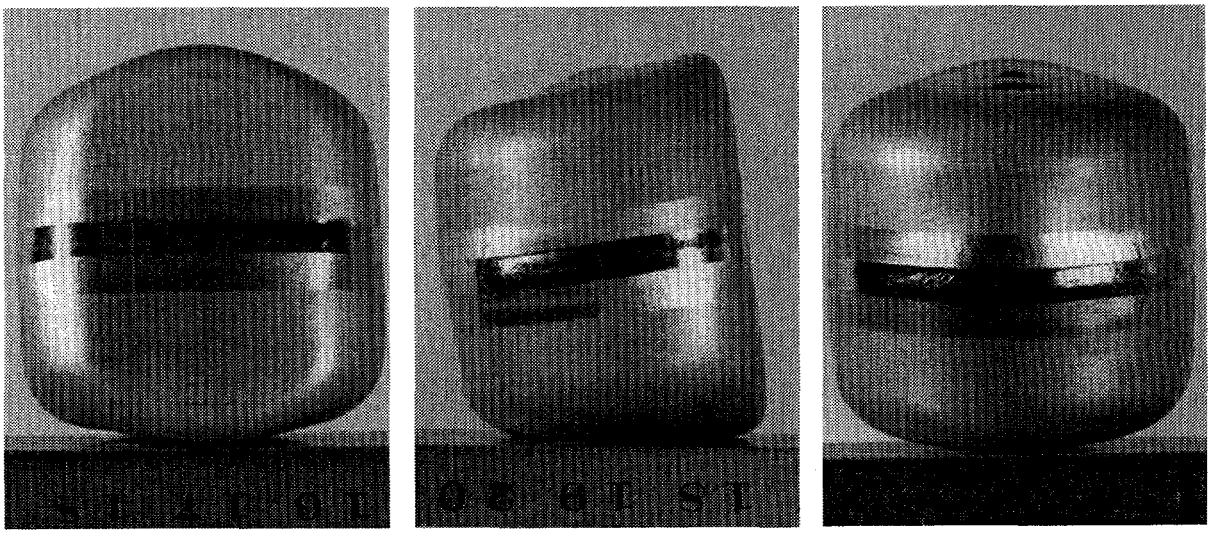

(a) (b) (c)

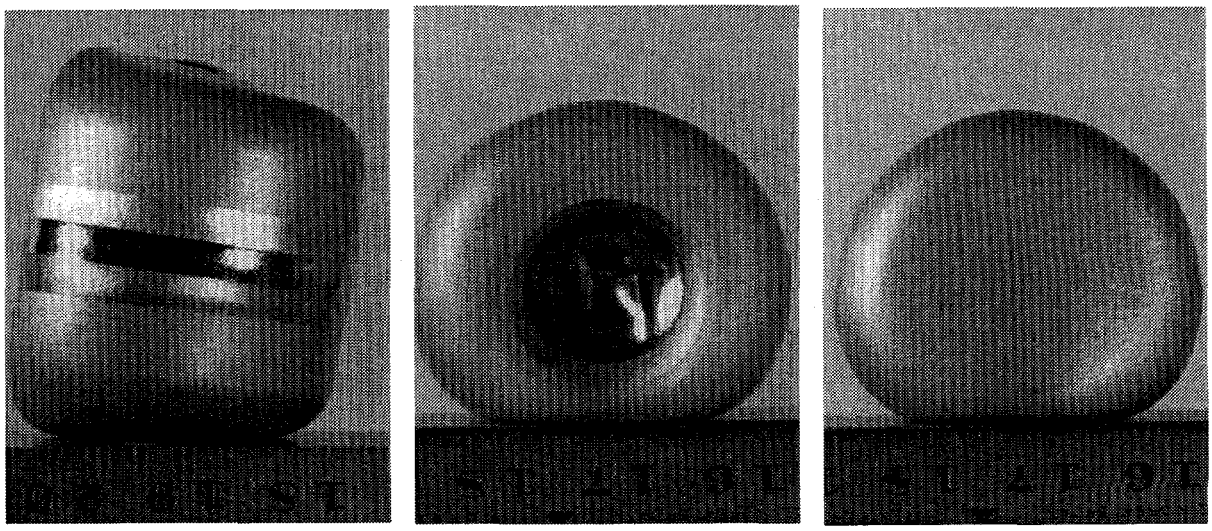

(d) (e) (f)

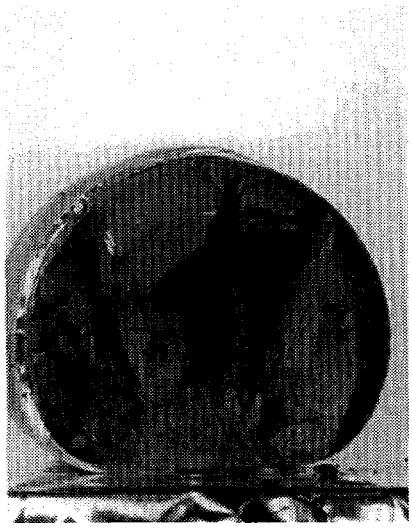

(g)

Figure 23. A small axial crack was observed on the trailing face of capsule SC0009. (a) impact face, (b) profile, (c) trailing face, (d) opposite profile, (e) vent end, (f) blind end, (g) fuel fragmentation. (NMT-9 Negs 941-74, 941-75, 941-73, 941-77, 941-76, 941-72, 941-78)

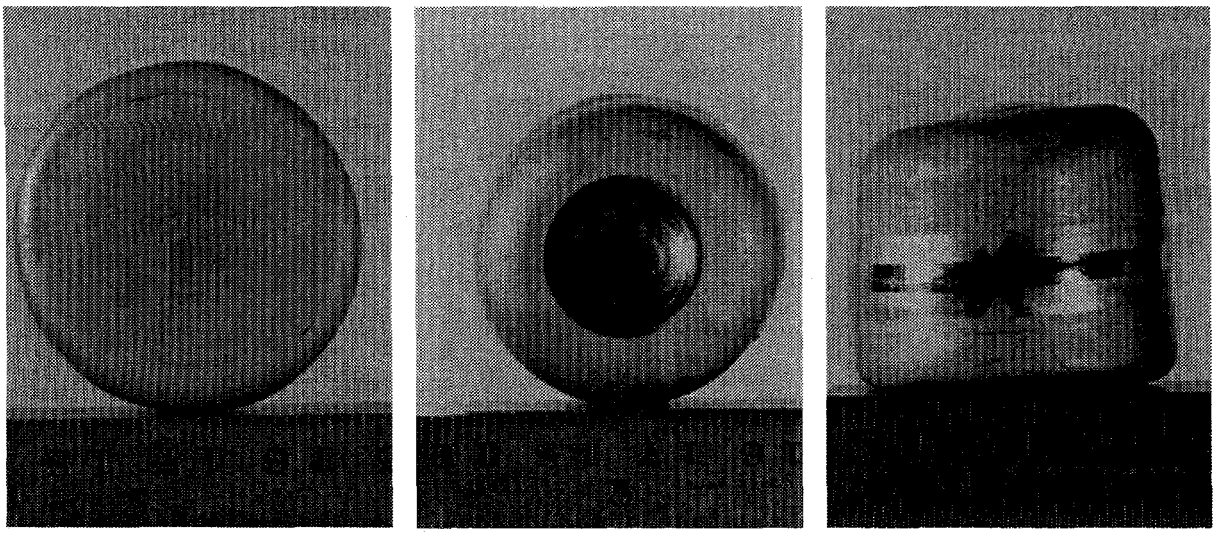

(a) (b) (c)

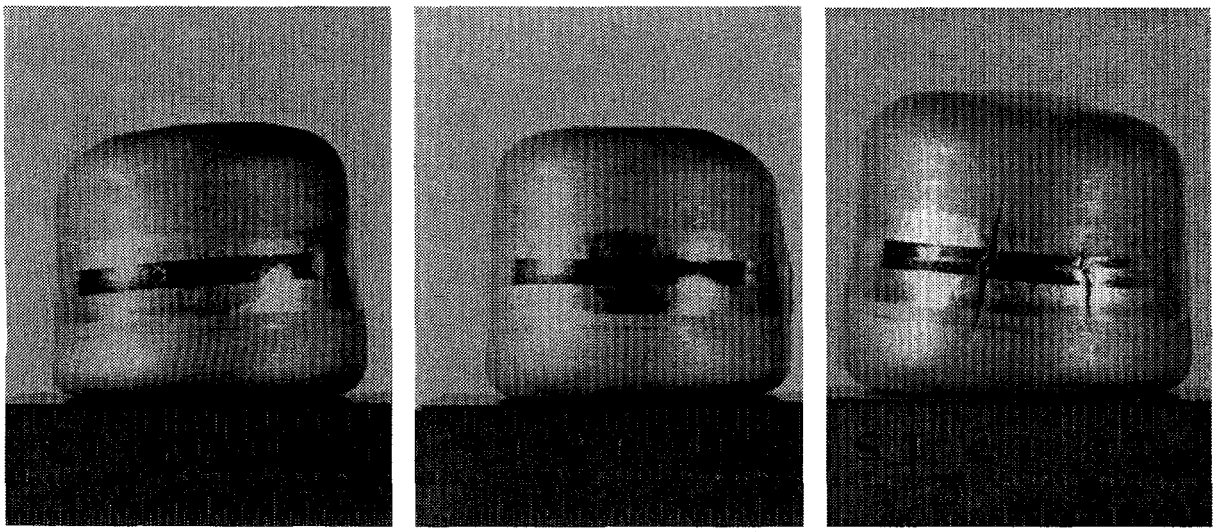

(d) (e) (f)

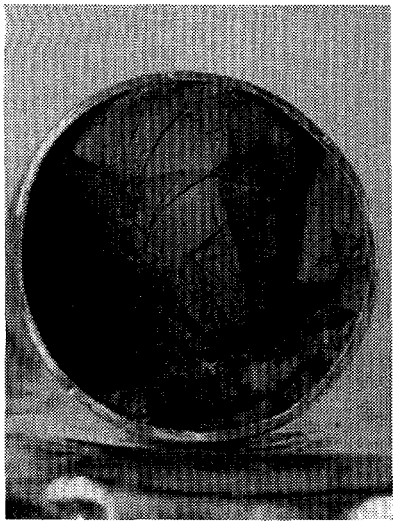

(g)

Figure 24. Capsule SC0016 was breached by two axial cracks at approximately 270 deg; (a) impact face, blind end, (b) vent end, (c) profile, 0 deg, (d) profile 90 deg, (e) profile 180 deg, (f) profile, 270 deg, (g) fuel fragmentation. (NMT-9 Negs 941-84, 941-80, 941-79, 941-81, 941-82, 941-83, 941-82-2)

The axial cracks measured approximately 11.8 mm and 6.7 mm in length. The longest crack had a maximum width of approximately 1.4 mm located just above the weld centerline. The width of the smaller axial crack , located just below the weld in the shield cup, measured approximately 0.4 mm. The weld shield was intact between the clad and the pellet and probably prevented the release of any urania from the capsule. Examination of these cracks revealed intergranular failure with a small amount of radial displacement and wall thinning (Fig. 25). The lack of any other microstructural evidence suggests that the cracks were not caused by anything other than pellet fragmentation displacement.

Examination of the single-pass and weld overlap regions revealed typical microstructures. Average vent and shield cup wall grain sizes are listed in Table X.

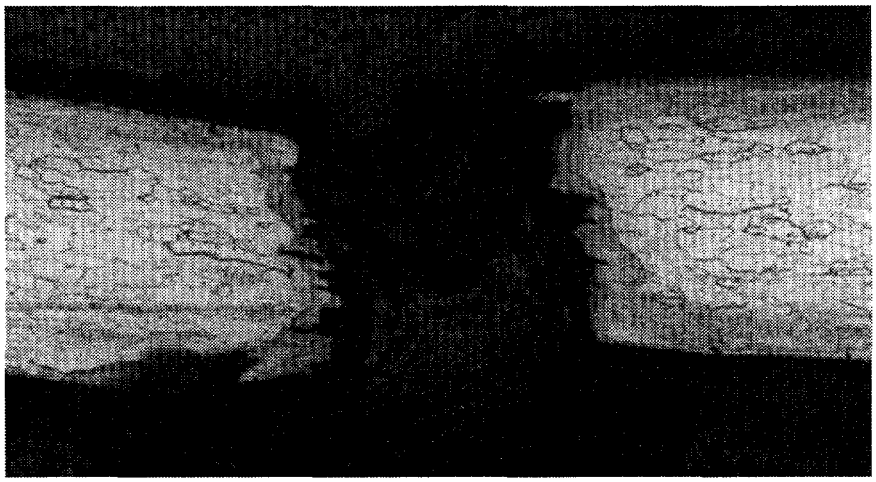

Figure 25. Axial crack in SC0016; etched, at 50× magnification. (NMT-9 Neg 943-89)

L. CPV-12

The module, containing capsules loaded with cold-pressed and sintered urania pellets, was impacted against a 25.4-mm-thick structural steel plate target at 54.38 ± 0.07 m/s and 970°C. The test components and loading orientation are listed in Table I. The module was intact. Two large cracks, each centered along the GIS cavity axis, were observed on the flight control surface/impact face (Fig. 26). One large longitudinal crack was observed in the surface opposite the impact face. One GIS was ejected from the module. No urania was detected in the catch tube. The capsule strains are listed in Table VI. The particle size analysis results of the one opened capsule (SC0074) are given in Table IX.

The A GIS was ejected from the module and was intact (Fig. 27). The clad loaded in the open end of this GIS (SC0073) was also ejected, whereas the clad loaded in the blind end remained in place. A large axial crack extending approximately 80% of the GIS's length was located opposite the impact surface of the GIS. The C GIS was intact with an axial crack extending along approximately 80% of the its length. The end cap was in place but was cracked in half.

No visible cracks or breaches were observed in any of the impacted clads. The impact face was centered at 0 deg for SC0073 (Fig. 28), at approximately 270 deg for SC0072 (Fig. 29),

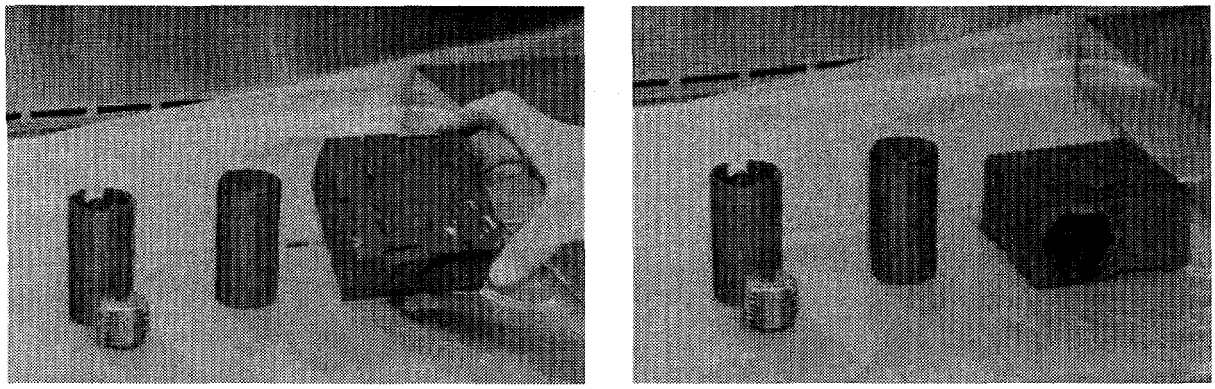

(a) (b)

Figure 26. Module and GISs impacted in CPV-12; (a) GIS A, SC0073 in front, GIS C, impact face of module, left to right, (b) GIS A, SC0073 in front, GIS C, trailing face of module, left to right. (NMT-9 Negs B2126-30 and B2126-29)

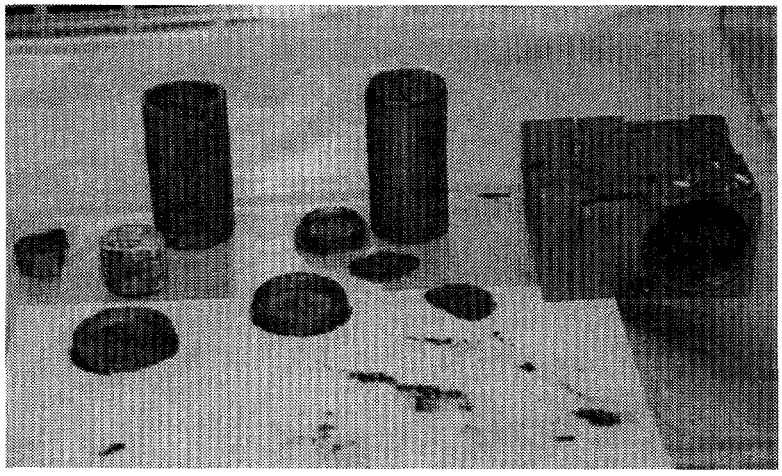

(a)

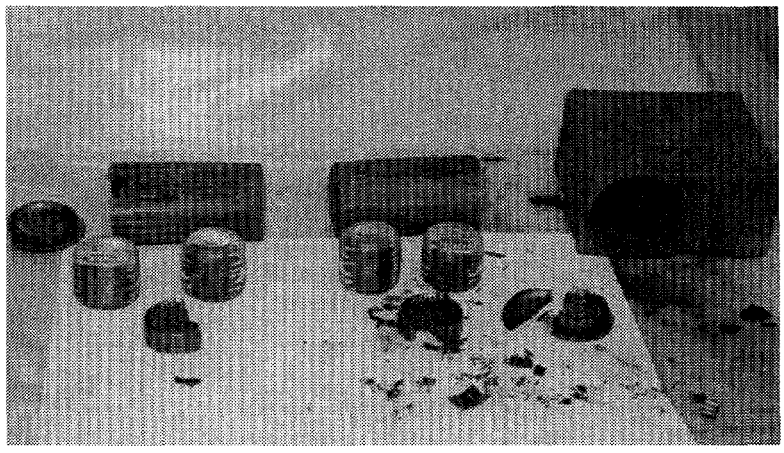

(b)

Figure 27. Module and GISs impacted in CPV-12; (a) GIS A , SC0073 in front, GIS C, impact face of module, left to right, (b) GIS A, SC0072 and SC0073 in front, GIS C, SC0075 and SC0074 in front, trailing face of module, left to right. (NMT-9 Negs B2126-32 and B2126-37)

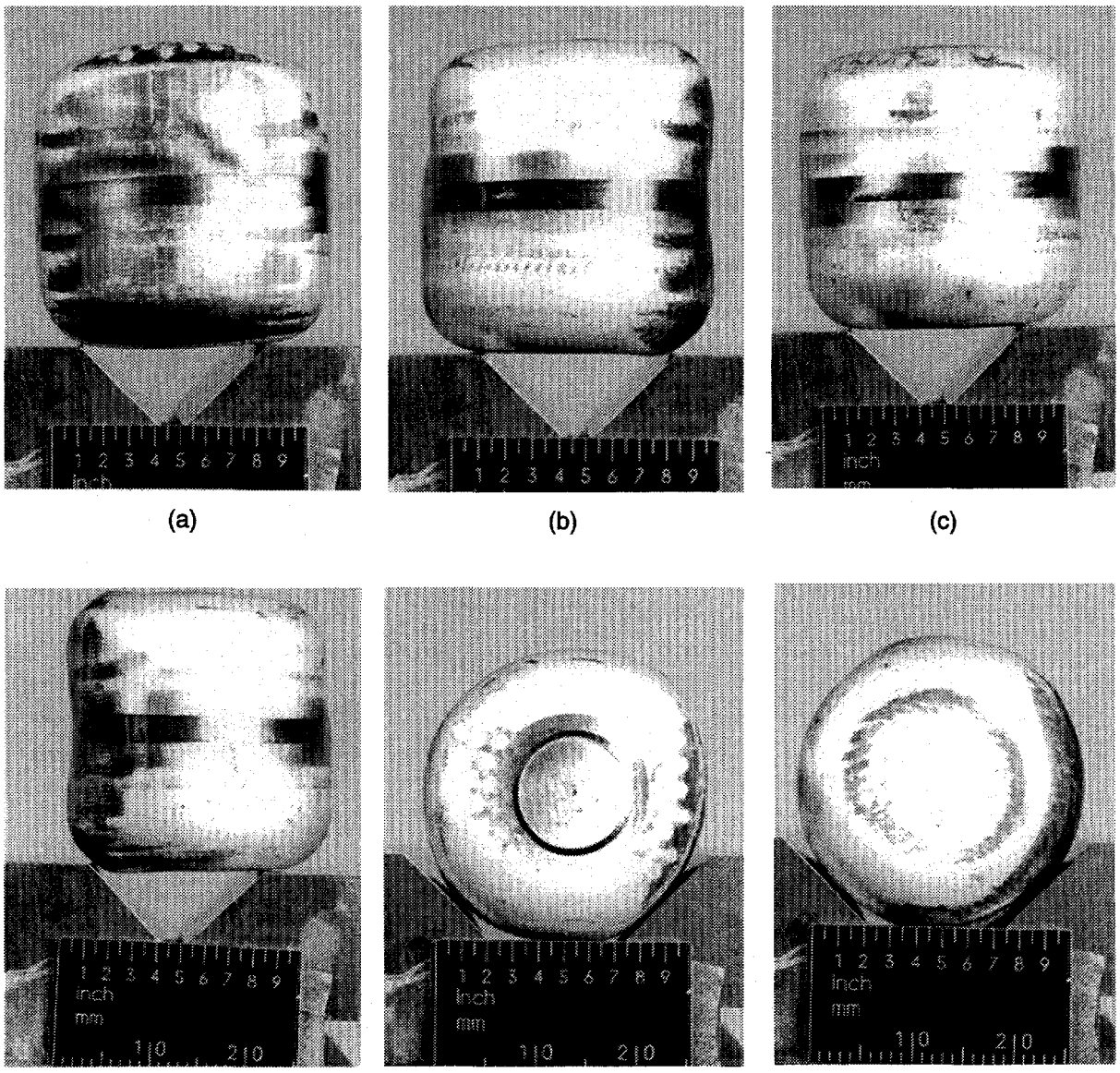

Figure 28. The impact face of SC0073 (GIS A, blind end) was centered at approximately 0 deg. (a) impact face, (b) profile, (c) trailing face, (d) opposite profile, (e) vent end, (f) blind end. (NMT-9 Negs 954-90, 954-91, 954-92, 954-93, 954-94, 954-95)

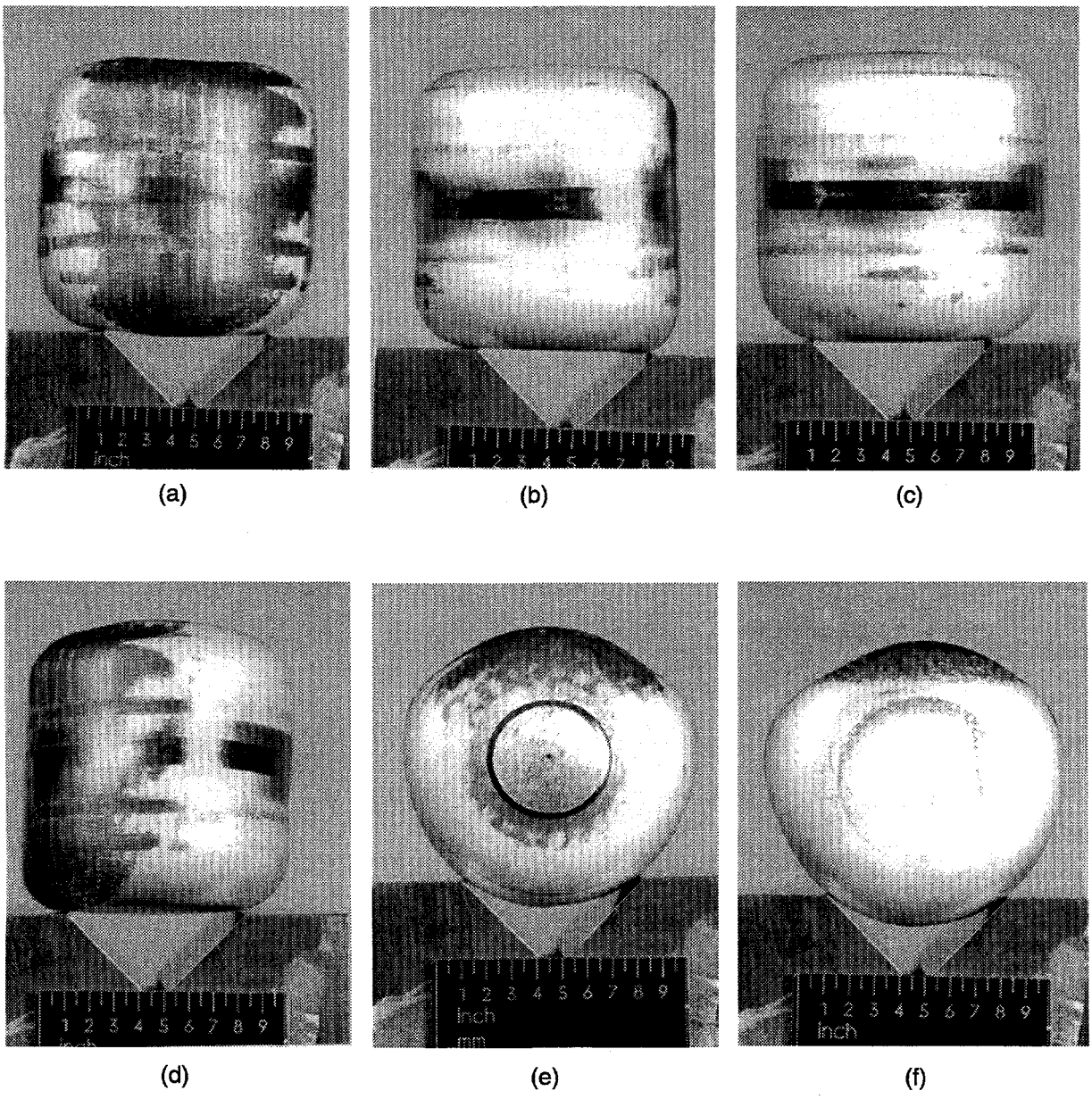

Figure 29. The impact face of SC0072 (GIS A, open end) was centered at approximately 270 deg. (a) impact face, (b) profile, (c) trailing face, (d) opposite profile, (e) vent end, (f) blind end. (NMT-9 Negs 954-87, 954-84, 954-85, 954-86, 954-88, 954-89)

at approximately 180 deg for SC0074 (Fig. 30), and at approximately 300 deg for SC0075 (Fig. 31), where 0 deg is the weld start and the rotation angle is clockwise with the vent facing up. The amount of deformation was very similar for each clad. On the trailing faces of the clads, ridges were observed that appeared to have been caused by fragmentation and displacement of the pellet fragments.

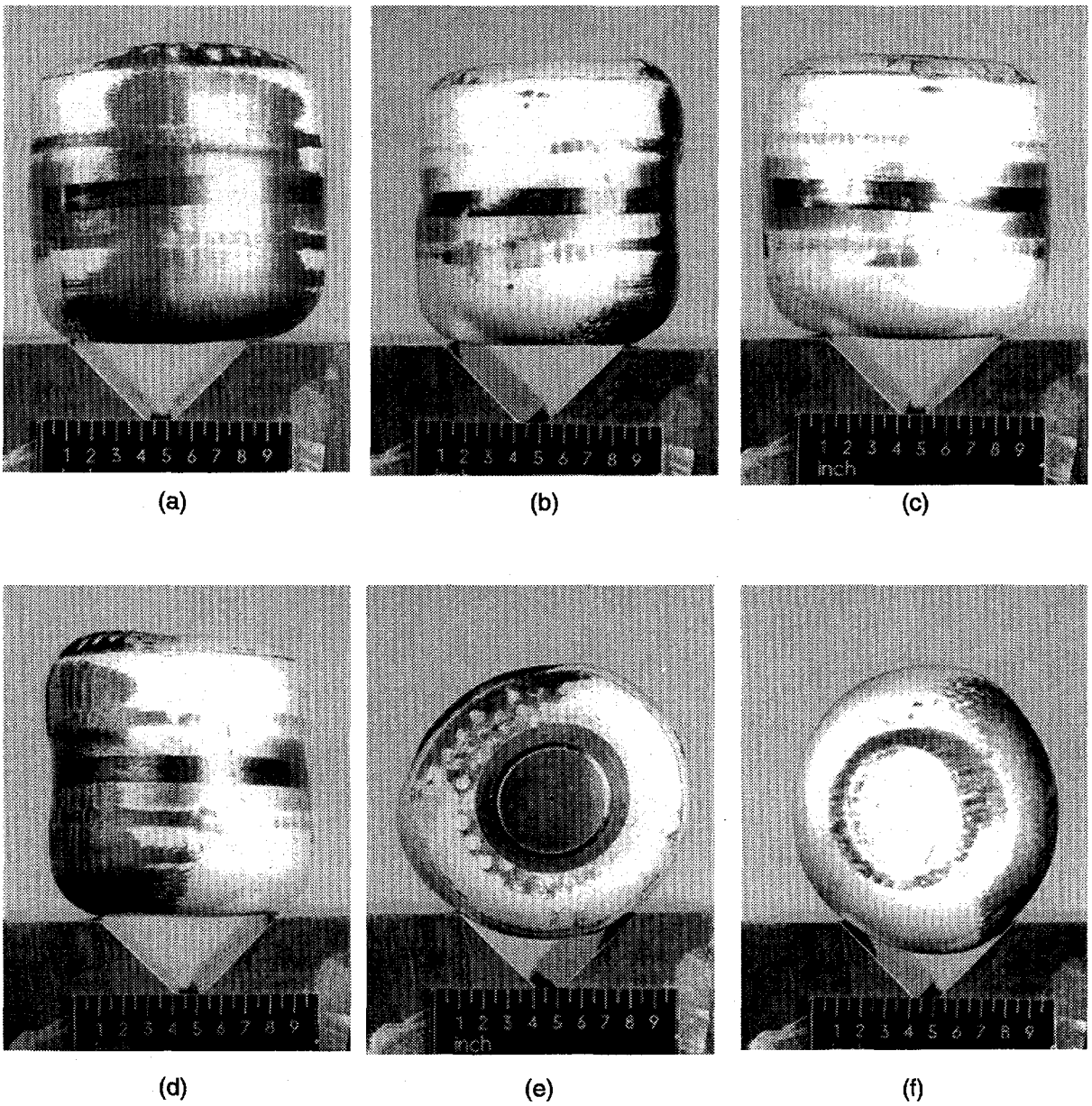

Figure 30. The impact face of SC0074 (GIS C, blind end) was centered at approximately 180 deg. (a) impact face, (b) profile, (c) trailing face, (d) opposite profile, (e) vent end, (f) blind end. (NMT-9 Negs 954-98, 954-99, 954-96, 954-97, 955-1, 955-2)

Capsule SC0074 was the most severely strained of the four clads (Table VI) and was therefore chosen for opening and for metallographic examination. Upon opening the clad, the observed fuel fragmentation appeared to have occurred radially from the impact face (Fig. 32). No anomalies were observed in any of the six sections removed for examination. Examination of the weld overlap and single-pass weld regions revealed exemplary microstructure (Fig. 33). The vent area microstructure was typical and did not have any unusual features.

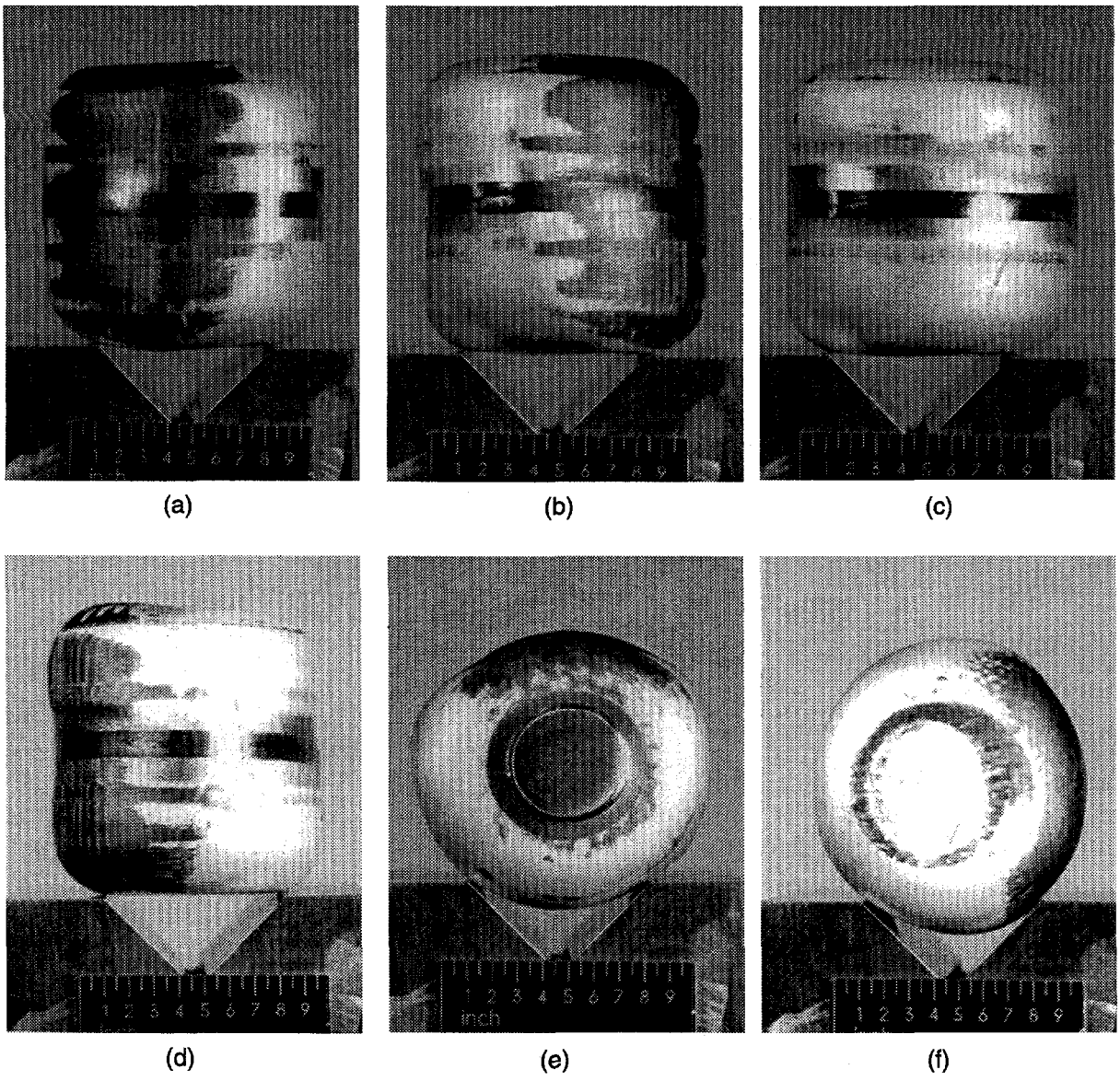

Figure 31. The impact face of SC0075 (GIS C, open end) was centered at approximately 300 deg. (a) impact face, (b) profile, (c) trailing face, (d) opposite profile, (e) vent end, (f) blind end. (NMT-9 Negs 955-6, 955-3, 955-4, 955-5, 955-7, 955-8)

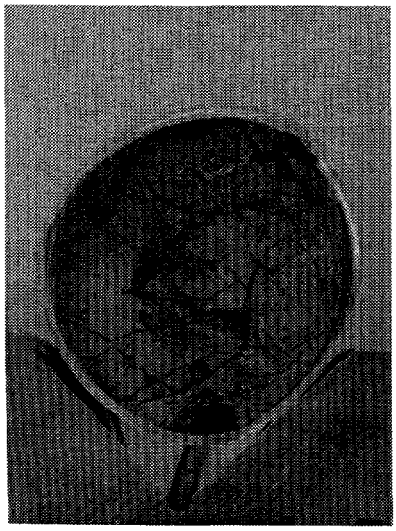

Figure 32. Fuel fragmentation pattern of SC0074. (NMT-9 Neg SC74-F)

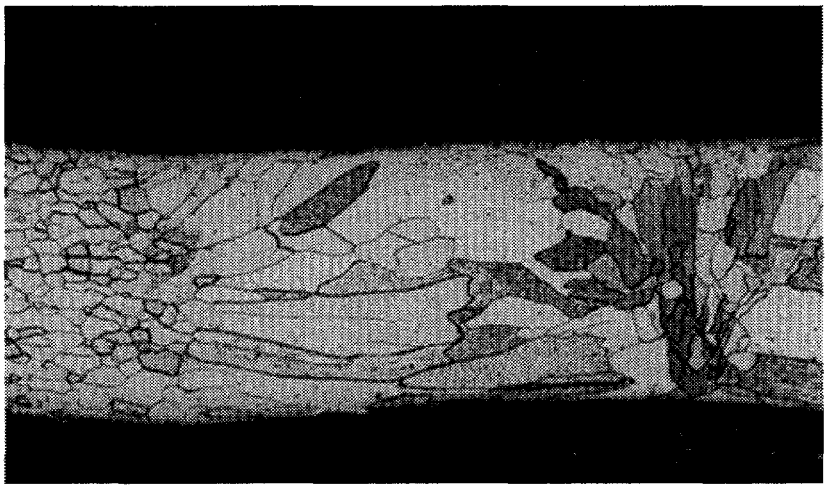

(a)

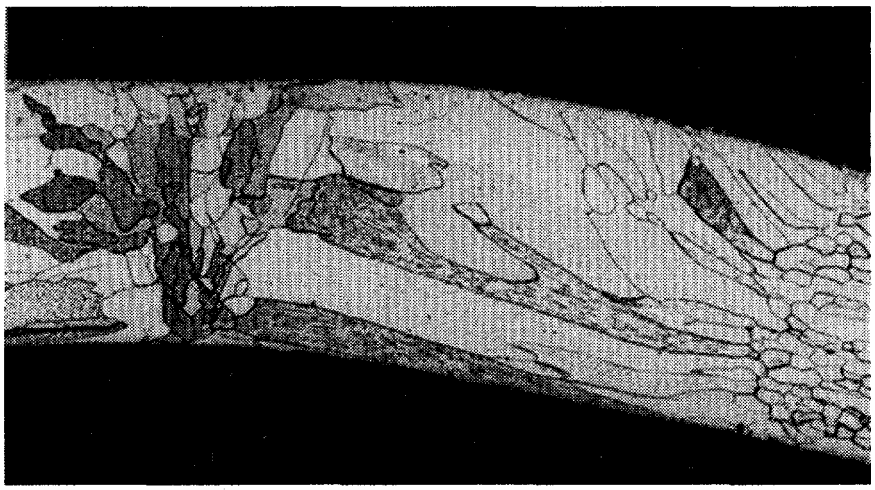

(b)

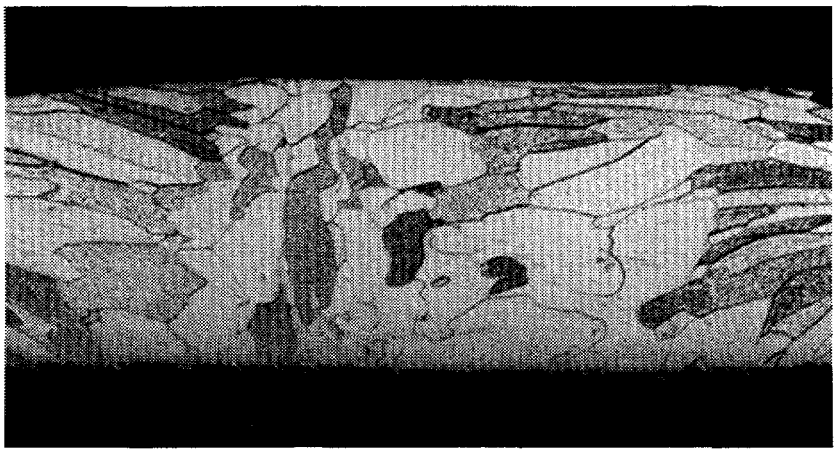

(c)

Figure 33. Capsule SC0074 weld microstructure; (a) and (b) single-pass region, etched, at 50× magnification; (c) weld overlap region, etched, at 50× magnification. (NMT-8 Negs 9510-54, 9510-55, 9510-56)

V. DISCUSSION

A. Impact Repsonse

Of the GPHS capsules tested in the bare-clad impacts with the capsule equator oriented perpendicular to the target (CPVs 1–10), 60% had cracks that breached the iridium cladding. Of these failures, four were in capsules loaded with hot-pressed pellets, and four were in capsules loaded with cold-pressed and sintered pellets. The one bare-clad impact test with the capsule equator oriented parallel to the target, CPV-11, resulted in a breach, however, no urania release was detected. A total of 67% of the breached capsules resulted in detectable urania releases.

No clad failures were observed in the single-module impact, CPV-12. The levels of capsule deformation observed in this test were generally much lower than strains observed with similar impacts in the Safety Verification Test (SVT) series.[6-8]

Metallographic examination of cracks in the tested capsules revealed typical intergranular failures. Slight wall thinning was also noted in a few of the breached areas. This compares well with iridium failures observed in the Design Iteration Test (DIT) and SVT test series.[1-8] All of the observed failures in the CPV capsules appeared to be related to displacement of pellet fragments and subsequent push-through. No significant anomalies were observed in the weld, vent, or capsule wall microstructures. In fact, the minor anomalies that were observed (the vent and shield cup wall offset in CPV-1 capsule, the weld-weld shield fusion in CPV-2 capsule, and the weld overlap area bulge in CPV-9 capsule) apparently had no effect on capsule impact performance.

B. Fines Generation

Based on data presented in Tables VII through IX, there appears to be no marked difference between the particle size profiles of the impacted cold-pressed and sintered urania pellets and the hot-pressed pellets. The weight fractions in each particular particle size range overlap. For example, the weight fraction within the +2000 to 5600 μm range varies from 0.1770 to 0.4550 in the hot-pressed pellets impacted in tests CPV-1, -2, -9, -10, and -11. The weight fraction of material within the identical size range varies from 0.2439 to 0.3482 in tests of cold-pressed and sintered pellets (CPV-3 through -8). In the ±10 μm size range, the weight fractions vary from 0.0053 to 0.0159 in hot-pressed pellet impacts and from 0.0044 to 0.0184 in bare-clad impacts with cold-pressed pellets. On the basis of fines generation, there is no way to differentiate between the two types of pellets impacted in this test series.

C. Impact Response and Fines Generation—Comparison to Previous Data

Table XII lists the particle size distributions of four simulant-fueled GPHS capsule bare-clad impact (BCI) tests conducted in support of the Galileo and Ulysses missions. Tests BCI-8 and -9 had capsule breaches with urania release, whereas tests BCI-6 and -10 did not. The capsules were impacted at 54 m/s and 1091°C. The particle size distributions of the recovered urania fuel are very similar for tests BCI-6, -8, and -10. The distribution of BCI-9 differs from the others significantly and may represent an experimental outlier. The disparity cannot be attributed to capsule failure, as the distribution of BCI-8 fuel is similar to that of BCI-6 and -10. No explanation was identified for the dissimilarity.

Table XII. Particle Size Distribution of Simulant BCI Tests[a]

Particle Size Range (μm)	TEST ID[b] BCI-6	BCI-8	BCI-9	BCI-10
+5600	0.56415	0.55013	0.82268	0.50690
+2000 to 5600	0.14896	0.22591	0.04819	0.21974
+850 to 2000	0.11707	0.13351	0.06399	0.16213
+425 to 850	0.07548	0.04220	0.03419	0.06231
+180 to 425	0.04939	0.02550	0.01990	0.02951
+125 to 180	0.01290	0.00510	0.00270	0.00580
+75 to 125	0.01110	0.00560	0.00340	0.00430
+45 to 75	0.00610	0.00320	0.00150	0.00240
+30 to 45	0.00460	0.00230	0.00090	0.00170
+20 to 30	0.00180	0.00100	0.00050	0.00080
+10 to 20	0.00340	0.00170	0.00060	0.00110
+9 to 10	0.00048	0.00036	0.00016	0.00051
+8 to 9	0.00102	0.00037	0.00030	0.00104
+7 to 8	0.00114	0.00040	0.00025	0.00043
+6 to 7	0.00072	0.00021	0.00017	0.00023
+5 to 6	0.00021	0.00028	0.00009	0.00011
+4 to 5	0.00022	0.00056	0.00008	0.00013
+3 to 4	0.00023	0.00048	0.00009	0.00010
+2 to 3	0.00019	0.00021	0.00006	0.00016
+1 to 2	0.00050	0.00058	0.00007	0.00000
<1	0.00034	0.00040	0.00018	0.00060
TOTAL:	1.00000	1.00000	1.00000	1.00000
Weight Fraction <10 μm:	0.00505	0.00385	0.00145	0.00331

[a]Data obtained from GPHS Safety Tests, Particle Size Data Package, LACP-86-62, compiled by Dan Pavone, Los Alamos National Laboratory. Limited Distribution.

[b]Impact velocities of BCI-6,-8 ,-9, and -10 were 54.34, 54.50, 54.48, and 54.19 m/s respectively.

In general, the following observations can be made regarding the fragmentation response of the BCI tests compared to that of the CPV tests. It appears that fines generation is slightly greater in the CPV than in the BCI tests. Table XIII compares the urania fragmentation of clads that breached and Table XIV compares nonbreaching clads.

Among the breached clads, the weight fraction of material in the ±10 μm range is roughly two to three times greater in the CPV capsules than in the BCI capsules. However, it is not clear whether this slight increase in fines generation is significant on a statistical or on an absolute basis. The weight fraction of urania in the range of +20 to 45 is from twice to an order of magnitude smaller in the CPV tests than in the BCI tests. This is probably not significant, because the weight fraction ±10 μm is larger than the +20 to 45 range, thereby accounting for a larger amount of material.

Similar trends were noted for the unbreached clads. The weight fraction of material in the ±10 μm range is roughly two to four times greater in the CPV capsules than in the BCI capsules. The weight fraction of urania in the range of +30 to 45 is from four to seven times smaller in the CPV tests than in the BCI tests.

TABLE XIII. Comparison of Pellet Fragmentation in Breached Bare Clad Impact Clads.

	WEIGHT FRACTION					
Particle Size			***Hot-Pressed Pellets***		***Cold-Pressed Pellets***	
Range (μm)	**BCI-8**	**BCI-9**	**CPV-1**	**CPV-9**	**CPV-4**	**CPV-5**
+180	0.9773	0.9890	0.9499	0.9876	0.9674	0.9671
+125 to 180	0.0051	0.0027	0.0225	0.0026	0.0065	0.0039
+75 to 125	0.0056	0.0034	0.0026	0.0018	0.0071	0.0040
+45 to 75	0.0032	0.0015	0.0018	0.0016	0.0055	0.0031
+30 to 45	0.0023	0.0009	0.0009	0.0000	0.0002	0.0006
+20 to 30	0.0010	0.0005	0.0014	0.0000	0.0001	0.0017
+10 to 20	0.0017	0.0006	0.0047	0.0003	0.0015	0.0073
≤10	0.0039	0.0015	0.0161	0.0061	0.0116	0.0122
TOTAL	1.0000	1.0000	1.0000	1.0000	1.0000	1.0000

TABLE XIV. Comparison of Pellet Fragmentation in Nonbreached Bare Clad Impact Clads.

	WEIGHT FRACTION				
Particle Size			***Hot-Pressed Pellets***	***Cold-Pressed Pellets***	
Range (μm)	**BCI-6**	**BCI-10**	**CPV-2**	**CPV-3**	**CPV-8**
+180	0.9551	0.9806	0.9860	0.9605	0.9796
+125 to 180	0.0129	0.0058	0.0016	0.0033	0.0019
+75 to 125	0.0111	0.0043	0.0016	0.0046	0.0021
+45 to 75	0.0061	0.0024	0.0016	0.0022	0.0011
+30 to 45	0.0046	0.0017	0.0000	0.0007	0.0012
+20 to 30	0.0018	0.0008	0.0000	0.0020	0.0018
+10 to 20	0.0034	0.0011	0.0006	0.0083	0.0052
≤10	0.0051	0.0033	0.0086	0.0184	0.0071
TOTAL	1.0000	1.0000	1.0000	1.0000	1.0000

D. Relationship Between UT Weld Evaluations and Impact Response

Ultrasonic testing is used to nondestructively evaluate each GPHS girth weld. The test method utilizes a standard with machined slots to calibrate the instrument in order to relate reflected signal magnitude to a defect size. Ultrasonic testing detects geometric anomalies (e.g., a crack, void, or wall-thickness mismatch) and reports the signal magnitude, as calibrated, in equivalent mils.

Table XI lists the maximum UT indications and their locations along with the actual location of the weld failure, if there was one. Of the eight "reject" capsules impacted, two did not fail and six did. All weld failures occurred at locations other than the locations of maximum UT indications. It should also be noted that none of these weld failures were related to the presence of weld defects; all of the failures propagated from other areas into the weld or resulted from pellet fragmentation and push-through. Of the seven "accept" capsules, six capsules experienced no failures and one contained a breaching crack (but no detectable urania was released).

VI. CONCLUSIONS

1. There appears to be no significant difference between the fragmentation characteristics of the hot-pressed and the cold-pressed and sintered urania pellets used in this study.

2. Anomalies that were observed in the capsules—cup wall offset in weld area, weld-weld shield fusion, and weld overlap bulge—did not have any effect on capsule impact response.

3. The levels of capsule deformation observed in the full module impact (CPV-12) were significantly lower than those observed in similar impacts in the SVT test series.

4. Generally, generation of ≤10 μm fines was slightly greater in the CPV test series than in previous simulant-fueled bare clad impact tests.

5. Results of the ultrasonic test evaluation of the girth weld could not be correlated with capsule impact response.

VII. ACKNOWLEGMENTS

We thank C. Frantz, A. Herrera, and W. Bast for conducting the impact tests and T. Baros, E. Burciaga, C. Lynch, P. Moniz, and M. Padilla for performing metallography, sample preparation, and particle size analyses.

REFERENCES

1. F. W. Schonfeld, "General-Purpose Heat Source Development: Safety Test Program, Postimpact Evaluation, Design Iteration Test 1," Los Alamos National Laboratory report LA-9680-SR (April 1984).

2. F. W. Schonfeld and T. G. George, "General-Purpose Heat Source Development: Safety Test Program, Postimpact Evaluation, Design Iteration Test 2," Los Alamos National Laboratory report LA-10012-SR (June 1984).

3. F. W. Schonfeld and T. G. George, "General-Purpose Heat Source Development: Safety Test Program, Postimpact Evaluation, Design Iteration Test 3," Los Alamos National Laboratory report LA-10034-SR (July 1984).

4. T. G. George and F. W. Schonfeld, "General-Purpose Heat Source Development: Safety Test Program, Postimpact Evaluation, Design Iteration Test 4," Los Alamos National Laboratory report LA-10217-SR (December 1984).

5. T. G. George and F. W. Schonfeld, "General-Purpose Heat Source Development: Safety Test Program, Postimpact Evaluation, Design Iteration Test 5," Los Alamos National Laboratory report LA-10232-SR (December 1984).

6. D. Pavone, T. G. George, and C. E. Frantz, "General-Purpose Heat Source Safety Verification Test Series: SVT-1 Through SVT-6," Los Alamos National Laboratory report LA-10353-MS (June 1985).

7. T. G. George and D. Pavone, "General-Purpose Heat Source Safety Verification Test Series: SVT-7 Through SVT-10," Los Alamos National Laboratory report LA-10408-MS (September 1985).

8. T. G. George and D. Pavone, "General-Purpose Heat Source Safety Verification Test Series: SVT-11 Through SVT-13," Los Alamos National Laboratory report LA-10710-MS (May 1986).

9. T. G. George, R. E. Tate, K. M. Axler, "General-Purpose Heat Source Development: Safety Verification Test Program; Bullet/Fragment Test Series," Los Alamos National Laboratory report LA-10364-MS (May 1985).

10. T. G. George, "General-Purpose Heat Source Development: Safety Verification Test Program; Titanium Bullet/Fragment Test Series," Los Alamos National Laboratory report LA-10724-MS (June 1986).

11. T. A. Cull, T. G. George, and D. Pavone, "General-Purpose Heat Source Development: Safety Verification Test Program; Explosion Overpressure Test Series," Los Alamos National Laboratory report LA-10697-MS (September 1986).

12. T. A. Cull and D. Pavone, "General-Purpose Heat Source Development: Safety Verification Test Program; Flyer Plate Test Series," Los Alamos National Laboratory report LA-10742-MS (September 1986).

13. T. G. George, "General-Purpose Heat Source Development: Safety Verification Test Program; Edge-On Flyer Plate Tests," Los Alamos National Laboratory report LA-10872-MS (March 1987).

Los Alamos
NATIONAL LABORATORY
Los Alamos, New Mexico 87545